

Co-Editor Decision: Reconsider after major revisions (23 Oct 2018) by Alma Hodzic

Comments to the Author:

Dear Authors,

I have not received your response to the report of the 3rd reviewer. Could you please address the reviewer's concerns:

RESPONSE: Dear Editor, you claim that you did not receive a response to the report of the 3rd reviewer; however, we never received any notification for any additional review. Please have a look at the interactive discussions of the manuscript (<https://www.atmos-chem-phys-discuss.net/acp-2018-94/#discussion>). I suppose that this is not our mistake. Nevertheless, we answer the question below.

This manuscript approaches a very interesting topic, increasing fire frequency in high latitude peatlands and the influence of peat fire atmospheric emissions on radiative forcing and climate change through deposition on high albedo surfaces such as snow and ice. However, I believe that the manuscript takes a totally misguided approach by focusing on BC emissions because peat fires burn almost exclusively with smoldering combustion that does not emit BC but large quantities of OC (as shown in the cited emission factors of Agaki et al., 2011 with OC emission factors being a factor of 30 larger than those of BC). Therefore, it is general knowledge that aerosol light absorption by smoke from peat fires is largely caused by BrC, not by BC. Therefore, I suggest that the authors refocus their manuscript on BrC and examine its radiative forcing and compare it to that of BC. Below, I've given a number of relevant publications to help the authors get started with this. In addition, the modification of the spectral reflectivity of snow through the deposition of peat combustion smoke has recently been discussed (Beres and Moosmüller, 2018).

RESPONSE: Although the topic of the paper is to study BC emitted from the 2017 fires in Greenland, we have corrected the whole manuscript and made several additional simulations to include OC and BrC as a sign of good will in order to finally complete this initially intended fast-track publication that was first submitted 1 year ago.

As you may notice from the results, including impact of BrC does not change a lot the impact of the emitted substances to the Greenland Ice Sheet.

REFERENCES

Akagi, S. K., Yokelson, R. J., Wiedinmyer, C., Alvarado, M. J., Reid, J. S., Karl, T., Crouse, J. D. and Wennberg, P. O.: Emission factors for open and domestic biomass burning for use in atmospheric models, *Atmos. Chem. Phys.*, 11(9), 4039–407doi:10.5194/acp-11- 4039-2011, 2011.

Beres, N. D. and H. Moosmüller (2018). Apparatus for Dry Deposition of Aerosols on Snow. *Atmos. Meas. Tech. Discuss.*, doi.org/10.5194/amt-2018-194, *Atmos. Meas. Tech.*, in review.

Black, R. R., J. Aurell, A. Holder, I. J. George, B. K. Gullett, M. D. Hays, C. D. Geron, and D. Tabor (2016), Characterization of Gas and Particle Emissions from Laboratory Burns of Peat, *Atmos. Environ.*, 132, 49-57.

Bhattacharai, C., V. Samburova, D. Sengupta, M. Iaukea-Lum, A. C. Watts, H. Moosmüller, and A. Y. Khlystov (2018), Physical and Chemical Characterization of Aerosol in Fresh and Aged Emissions from Open Combustion of Biomass Fuels, *Aerosol Sci. Tech.*, DOI: 10.1080/02786826.2018.1498585.

Chakrabarty, R. K., H. Moosmüller, L.-W. A. Chen, K. Lewis, W. P. Arnott, C. Mazzoleni, M. K. Dubey, C. E. Wold, W. M. Hao, and S. M. Kreidenweis (2010), Brown Carbon in Tar Balls from Smoldering Biomass Combustion, *Atmos. Chem. Phys.*, 10, 6363-6370.

Chakrabarty, R. K., M. Gyawali, R. L. N. Yatavelli, A. Pandey, A. C. Watts, J. Knue, L. W. A. Chen, R. R. Pattison, A. Tsiabart, V. Samburova, and H. Moosmüller (2016), Brown Carbon Aerosols from Burning of Boreal Peatlands: Microphysical Properties, Emission Factors, and Implications for Direct Radiative Forcing, *Atmos. Chem. Phys.*, 16(5), 3033-3040.

Lin, P., P. K. Aiona, Y. Li, M. Shiraiwa, J. Laskin, S. A. Nizkorodov, and A. Laskin (2016), Molecular Characterization of Brown Carbon in Biomass Burning Aerosol Particles, *Environ. Sci. Technol.*, 50(21), 11815-11824.

Samburova, V., J. Connolly, M. Gyawali, R. L. N. Yatavelli, A. C. Watts, R. K. Chakrabarty, B. Zielinska, H. Moosmüller, and A. Khlystov (2016), Polycyclic Aromatic Hydrocarbons in Biomass-Burning Emissions and Their Contribution to Light Absorption and Aerosol Toxicity, *Sci. Total Environ.*, 568, 391-401.

Sengupta, D., V. Samburova, C. Bhattarai, E. Kirillova, L. Mazzoleni, M. Iaukea-Lum, A. Watts, H. Moosmüller, and A. Khlystov (2018), Light Absorption by Polar and Non-Polar Aerosol Compounds from Laboratory Biomass Combustion, *Atmos. Chem. Phys.*, 18(15), 10849-10867.

Sumlin, B. J., Y. W. Heinson, N. Shetty, A. Pandey, R. S. Pattison, S. Baker, W. M. Hao, and R. K. Chakrabarty (2018), UV-Vis-IR Spectral Complex Refractive Indices and Optical Properties of Brown Carbon Aerosol from Biomass Burning, *Journal of Quantitative Spectroscopy and Radiative Transfer*, 206, 392-398.

Anonymous Referee #1

Review of “Open fires in Greenland: an unusual event and its impact on the albedo of the Greenland Ice Sheet” by N. Evangeliou and co-authors.

General comments.

N. Evangeliou and co-authors present a paper dealing with the atmospheric emission of black carbon by peat fires in Greenland during an extreme event in August 2017. They estimate the total amount of BC released in the atmosphere and its impact on the atmospheric radiative balance and snow albedo. The authors conclude that none of those impact are really significant. I found the paper lacking a focused scientific objective and finally it will have a limited interest for the scientific community. The methodology is sound but many of the assumptions must be clarify. The validation exercise is too qualitative while the dataset can be used for quantitative assessment. The conclusion that peat fire in Greenland could be of a significant importance for climate is not really supported by the findings of this paper.

Response: We agree that the methodology and parts of the discussion needed lots of improvement and we have made substantial effort with numerous changes in all parts of the manuscript according to both reviewers' suggestions (please see manuscript with Track Changes).

However, we do not agree with this description of our work. The validation is qualitative because no direct measurements of BC concentrations exist from this event occurring in a particularly data-sparse region, and also few satellite data document the event. The only data we found are Lidar data from CALIPSO that confirmed the presence of the plume where our model predicted it. Could the reviewer suggest, in concrete terms, which dataset could be used for quantitative assessment?

The reviewer says, “The conclusion that peat fire in Greenland could be of a significant importance for climate is not really supported by the findings of this paper.” This is NOT a conclusion, but a logical probability, considering that 25% of Greenland's surface is permafrost that is rich in peat. We now show this more clearly in the updated version of our manuscript. In addition, NASA's satellites show an increasing trend of fires in thawed permafrost over Greenland (**see new supplementary figure S1 or attached Fig. R1**) and our simulations showed that 30% of the emissions were deposited in the Greenland Ice Sheet (**Lines 388-391**).

We disagree with the comment of the reviewer that this paper will have a limited interest for the scientific community. We present some statistics from the ACP Discussions website.

In the Discussions page of the journal (https://www.atmos-chem-phys-discuss.net/discussion_papers.html), at the time that we started writing this response (22-05-2018), there are 30 papers in open discussion (ACPD) that were published the same time as ours (March 2018). If we calculate the average views and downloads we get **302±100 (min: 199 – max: 570)**, while our paper's visibility is **293**.

Furthermore, although media coverage does not converge with scientific quality, the present study was selected for a press conference on “Shape of things to come? The 2017 wildfire season” during the EGU 2018 conference (<https://client.cntv.at/egu2018/pc5>).

Specific comments.

Abstract

Line 43. Your conclusion doesn't support this fact and it's not scientifically based.

Response: Line 43 states "If the expected further warming of Greenland produces much larger fires in the future, this could indeed cause substantial albedo changes and thus lead to accelerated melting of the Greenland Ice Sheet." This sentence is NOT a conclusion, but a logical hypothesis (if). We have slightly rephrased the sentence, so it now reads: "If the expected future warming of the Arctic produces more fires in Greenland, this could indeed cause albedo changes and thus contribute to accelerated melting of the Greenland Ice Sheet." Finally, in order to prove that this is not pure speculation but a solid hypothesis, we support it with references (see last paragraph in conclusions).

Introduction.

The introduction is missing a comprehensive literature review on Arctic peat ecosystem and fire occurrence to better understand why those particular fires have been studied.

Response: We have focused our introduction on peatlands and fires in Greenland and think that a more comprehensive literature review on Arctic peat ecosystems in general is out of scope of this paper. After all, this paper studies the impact of fires in Greenland on BC concentration and deposition in Greenland, not on future scenarios of fire occurrence, permafrost melt or such.

Line 83-84. Provide evidence of the significance of this event compared to other events.

Response: Our statement that "... the fires ... , probably represent the largest fires that have occurred on Greenland in modern times.", is now supported by a new plot of the number of MODIS active fire detections (MODIS MCD14DL) over Greenland (**see new supplementary Figure S1 or attached Fig.R1**).

Method

L89-118. This section is very important as it is the starting point for the estimation of the BC amount released by fires. However the methodology used (eg. which sensor, when, spatial resolution, who and how has done the estimation, . . .) is unclear. On Line 241, we can read that the burnt surface area comes from GlobeCover 2009. So finally, what is your point?

Response: Line 241 has been corrected. We appreciate the reviewer for this constructive comment.

As regards to the methodology, we have done a few corrections to explain better what has been done, also giving specifications of the products we used (lines 97-99).

In our opinion, detailed explanations on the calculations are not needed, since the method has been already published in the relevant literature and used in many other previous cases. As we explain in the manuscript, the burned area was mapped using severity levels of dNBR index. The methodology of its application is described in details in Lutes et al. (2006) (pp. 201-270), which is **attached**. There is another paper describing how dNBR was calibrated in field - Escuin et al, 2008 (see reference in the manuscript). Since the index is sensitive to any disturbances, we applied a manually delineated fire perimeter to increase the accuracy of mapping.

You should rewrite this section with a detailed comment of Table 1 and explain how it compares to active fire mapping. Line 118 needs clarification based on quantitative information.

Response: Line 94 explicitly says that the location of the active fires were downloaded from NASA's website. So, what is shown in Table 1 has been confirmed with NASA's active fires (also shown in supplements' Figure S1 and attached Fig.R1).

Regarding to the severity levels (Line 118), qualitative information is given in Key and Benson (2006) together with all the details of the methodology used. The same methodology has been used to map the Chernobyl fires (see: Evangeliou et al., 2014; 2015; 2016)

The comment to confirm Line 118 based on quantitative information is too generic and we do not really understand what the reviewer wants us to do.

L155 Explain how you get this number and provide a range of possible values

Response: Line 155 says "In contrast, tropical peatlands can have deep burn depths of 40–50 cm and release an average of 300–450 t C ha⁻¹ (Page et al., 2015; Reddy et al., 2015)."

It should be obvious that this range of values was reported by Page et al. (2015) and Reddy et al. (2015).

If the reviewer means the average amount of organic fuel available for combustion that we used for the Greenland fires (100 t C ha⁻¹), it has been taken from Smirnov et al. (2015). In this paper, it was assumed that for peat-bog fires, the average amount of fuel available for combustion (including the soil organic matter) is up to 120 t/ha supported from measurements from IPCC (2006).

L180. Provide reference for BC density and size distribution. Peat fires emits large amount of organic carbon. The possible impact of the mixing state of BC and POM on aerosol size distribution, optical properties and residence time should be discuss in this paper.

Response: We agree that fires also emit large quantities of organic carbon (OC). However, the impact of OC on the albedo of the ice sheet is probably small, although it probably enhances the BC effect, since OC can also be slightly absorbing (e.g., brown carbon). But given the lack of information on the optical properties of the emitted OC, we think an additional analysis of OC would not be very meaningful.

With respect to BC density and size distribution, a reference was added in Line 214 of the updated manuscript. We have now also performed a sensitivity study on the impact of different particle size distributions on the deposition of BC over Greenland's Ice Sheet and discuss it in section 3.2. A detailed analysis of residence times of BC has been already presented by Grythe et al. (2017) [reference in the manuscript] and in Evangeliou et al. (2018) [reference under editorial check in ACP Discussions].

L200 and discussion section 3.3

The apportionment between emission from peat fires and other sources remains unclear for me. The methodology is not same as the one use for assessing impact of peat fire. The figure 4 is not really useful while other figures are in the supplement material.

Response: Lagrangian models such as the one used in our work (FLEXPARTv10) can run forward in time (like CTMs or climate models) using specific emissions that can be taken from an existing inventory (for example ECLIPSE, see:

http://www.iiasa.ac.at/web/home/research/researchPrograms/air/Global_emissions.html).

Moreover, Lagrangian models have the advantage that they can also run backward in time, from a specific point or region for which the user wants to calculate concentrations. What is produced then is the footprint emission sensitivity (or footprint), which is simply the residence time of the computational particles (in sec) in each grid-cell of the model. Then, by multiplying this footprint with a given emission inventory (e.g. ECLIPSE) given in kg/m²/s and dividing with the altitude of the lowest vertical level in the model, one obtains surface concentrations again. Notice that forward and backward calculations are equivalent, so the methodology is not different. However, depending on the setup, the computational efficiency can be much higher in backward mode, and that is also the reason we used it to assess the impact of emissions outside Greenland.

For FLEXPART that we used in this study, a comparison between forward and backward simulations can be found in Seibert and Frank (2004).

We calculate average concentrations of surface BC in four compartments of Greenland based on ECLIPSE emissions. ECLIPSE includes all anthropogenic sources, while we calculate biomass burning emissions using global MODIS-satellite hot spot data (Giglio et al., 2016) and GFAS (references in the manuscript). Everything is well documented in the associated references.

Figure 4 has been replaced by Figure S4 as suggested.

L204 and section 4.2

The methodology and the discussion section on RF computation must be improved and clearly states how you deal with both surface albedo and atmospheric effect of BC on the radiative balance. Figure 7 is confusing as it deals with both BOA, TOA, time series and geographical distribution as the same time.

Response: We have re-written and re-structured the whole chapter, both in the Methodology and analysis of the Results (see manuscript with Truck Changes). Our perception is not to present in detail methods that have been documented in previous publications. For RF calculations we used the uvspec model from the libRadtran radiative transfer software package (<http://www.libradtran.org/doku.php>) (see references in the manuscript: Emde et al., 2016; Mayer and Kylling, 2005). Snow albedo was calculated with the SNICAR model (<http://snow.engin.umich.edu/info.html>) in a two-layer configuration (see references in the manuscript: Flanner et al., 2007, 2009). These are open source codes that have been used by many groups worldwide. Figure 7 has been improved as suggested.

L218 and section 4.1 along with Figures 5 and 6. The validation exercise is really too qualitative and based on visual inspection of satellite data that are not really used scientifically. AERONET data can provide detailed information on aerosol optical properties and radiative forcing. CALIOP data products give aerosol extinction profiles which can be used in the RF computations.

Response: The reason the validation exercise is so qualitative is that we have no clear observations of the Greenland fire plume. The AERONET data show impacts of the forest fires burning outside Greenland. Only at one site, the AERONET data show an AOD increase that is partly (but not exclusively) due to the Greenland fires.

L466 Your last bullet point is rather speculative and not supported by the findings of the paper.

Response: This is true and we have now corrected it. The last bullet is NOT ALL OF IT a conclusion, but rather a comment and therefore, we now show it as a comment (not bulleted) below the bullet. We further support what we say in the sentence with references.

REFERENCES

- Lutes, Duncan C.; Keane, Robert E.; Caratti, John F.; Key, Carl H.; Benson, Nathan C.; Sutherland, Steve; Gangi, Larry J. 2006. FIREMON: Fire effects monitoring and inventory system. Gen. Tech. Rep. RMRS-GTR-164-CD. Fort Collins, CO: U.S. Department of Agriculture, Forest Service, Rocky Mountain Research Station. (ATTACHED)
- Key, C. H. and Benson, N. C.: Landscape assessment: Sampling and analysis methods, USDA For. Serv. Gen. Tech. Rep. RMRS-GTR-164-CD, (June), 1–55, doi:10.1002/app.1994.070541203, 2006.
- Evangelidou, N., Balkanski, Y., Cozic, A., Hao, W. M. and Møller, A. P.: Wildfires in Chernobyl-contaminated forests and risks to the population and the environment: A new nuclear disaster about to happen?, *Environ. Int.*, 73, 346–358, doi:10.1016/j.envint.2014.08.012, 2014.
- Evangelidou, N., Balkanski, Y., Cozic, A., Hao, W. M., Mouillot, F., Thonicke, K., Paugam, R., Zibtsev, S., Mousseau, T. A., Wang, R., Poulter, B., Petkov, A., Yue, C., Cadule, P., Koffi, B., Kaiser, J. W., Møller, A. P. and Classen, A. T.: Fire evolution in the radioactive forests of Ukraine and Belarus: Future risks for the population and the environment, *Ecol. Monogr.*, 85(1), 49–72, doi:10.1890/14-1227.1, 2015.
- Evangelidou, N., Zibtsev, S., Myroniuk, V., Zhurba, M., Hamburger, T., Stohl, A., Balkanski, Y., Paugam, R., Mousseau, T. A., Møller, A. P. and Kireev, S. I.: Resuspension and atmospheric transport of radionuclides due to wildfires near the Chernobyl Nuclear Power Plant in 2015: An impact assessment., *Sci. Rep.*, 6, 26062 [online] Available from: <http://www.nature.com/srep/2016/160517/srep26062/full/srep26062.html>, 2016.
- Smirnov, N. S., Korotkov, V. N. and Romanovskaya, A. A.: Black carbon emissions from wildfires on forest lands of the Russian Federation in 2007–2012, *Russ. Meteorol. Hydrol.*, 40(7), 435–442, doi:10.3103/S1068373915070018, 2015
- 2006 IPCC Guidelines for National Greenhouse Gas Inventories, Vol. 4: Agriculture, Forestry and Other Land Use (IPCC, 2006) [in Russian].
- Seibert, P. and Frank, A.: Source-receptor matrix calculation with a Lagrangian particle dispersion model in backward mode, *Atmos. Chem. Phys.*, 4(1), 51–63, doi:10.5194/acp-4-51-2004, 2004.
- Giglio, L., Descloitres, J., Justice, C. O. and Kaufman, Y. J.: An enhanced contextual fire detection algorithm for MODIS, *Remote Sens. Environ.*, 87(2–3), 273–282, doi:10.1016/S0034-4257(03)00184-6, 2003.

Anonymous Referee #2

General comments :

This work investigates the quantification of emissions of black carbon (BC) from intense fires on peat lands in Western Greenland during summer 2017 and their impacts on albedo reduction and radiative forcing. The authors conclude that those impacts of BC deposition of the Greenland Ice Sheet are almost negligible, which turns out to be a scientific result for the community. This study is interesting and sound for ACP. I have nevertheless several criticisms requiring a careful revision and in-depth improvements both in the methodology, often unclear, and in the discussion of the results before the paper is suitable for publication in ACP.

Response: We acknowledge the reviewer's comments and his effort to improve this manuscript. We have tried to follow his suggestions to correct the manuscript and have basically re-written parts of the manuscript (please see manuscript with Track Changes).

Specific comments :

L1-2 : The title seems to indicate that the main focus of the paper is the quantification of the reduction in albedo due to open fires in Greenland. Only ten lines in the paper really focus on the modification of the albedo due to BC deposition. The title should reflect the main findings of the paper : quantification of BC emissions of this unusual event, transport of the plume, deposition.

Response: We agree; we have changed the title to "Open fires in Greenland in summer 2017: transport and deposition of BC and impact on the Greenland Ice Sheet"

L41-44 and L496-500 : I find a bit strange to conclude both abstract and conclusion by something purely speculative and that does not match the main results of the paper.

Response: We admit that this is probably an extreme formulation and we have changed it to a weaker statement. We would like to draw attention that this statement is not a conclusion, but a logical hypothesis. To further show that it's not a conclusion, we now support the paragraph with references (see last paragraph in conclusions).

L83-84 : "the largest fires". Give maybe statistics or cite a climatological study to support this assertion.

Response: We have plotted the annual number of active fires from NASA's MODIS product in supplements' Figure S1 (or Fig.R1) starting from first year that satellite data were available (2001).

L111 : The authors should give more details about the procedure applied on the data. "Additional classification" is too vague.

Response: The statement has been removed!

L130 : "assuming a 6h persistence". How is this hypothesis justified ? Is it confirmed by observations or by other studies ?

Response: Well, this is confirmed by previous studies (Kaiser et al., 2012 – reference in the paper). We chose a persistence model similar to what is done in Kaiser et al. (2012) and used a time of the same order of magnitude with the mean return time of MODIS in the afternoon (peak time of fire) ~ 4h. For a description of the persistence model that was used, please see line 8 - page 9852 of Paugam et al. (2015).

L161 : Say clearly that the only variable computed in this study from measurements is the burned area A. The other factors are based on assumptions or provided by previous studies.

Response: Corrected. This is now explicitly mentioned in Line 184.

L181 : Those values suggest that aerosols are not only composed of BC (which is a reasonable assumption). How do the authors justify this size distribution ? It has indeed a huge influence on the deposition efficiencies (both sedimentation and wet removal) and on the calculation of aerosol optical properties. Both the radiative forcings and reduction of albedo on snow surfaces will be sensitive to this assumption on the size distribution. I suggest that the authors perform a sensitivity study on the influence of those parameters.

Response: After rapid coagulation, more than 90% of the mass of BC after fires is present in sizes between 0.1 – 1 μm in the atmosphere. This has been highlighted by many experiments/measurements and is now well justified in section 3.2.

However, we have followed the suggestion of the current reviewer and performed a sensitivity study using different size distribution of the BC particles produced from the 2017 fires in Greenland and we calculated the uncertainty on the deposited mass of BC due to different size distribution. We present and discuss the results at the end of section 3.2. The effect of different size distribution on residence times has been already studied by Grythe et al. (2017) [reference in the manuscript] and the different deposition coefficients in Evangeliou et al. (2018) [reference under editorial check in ACP Discussions].

The calculated uncertainty from this sensitivity test ranges from 10%–30% in 86% of the Sheet's surface to up to 50% in the rest of the Sheet's surface.

L200 : “a simple emission scheme”. What does it mean? Why don't the authors use the same methodology for all fires ?

Response: We appreciate reviewer's comment here. This was a typo error and we have updated this part of the methodology.

L200-201 : Those emission factors should depend on the type of soil and vegetation. Which maps have been used here ? Which values for emission factors have been finally chosen ? The reader should be able to reproduce the results of this study ; without such assumptions, it is impossible.

Response: Corrected; See previous comment.

Sect. 2.4 : Do the authors calculate radiative forcing assuming refractive index of BC only? The choice of the refractive index should be done in accordance with the size distribution (L181), which probably reflects an internal mixture of aerosols.

Response: The radiative forcing was calculated using the refractive index of BC only. We agree with the reviewer that BC was likely present as an internal mixture with other aerosol components (especially OC). However, we did not simulate OC and therefore used only the refractive index of BC. This will lead to an underestimation of the atmospheric effects of BC, since internal mixing with OC will likely enhance the BC absorption, and there may also be other absorbing components in the aerosol. However, we think that as an order of magnitude estimation of the atmospheric effects, our

assumption should be sufficient. Furthermore, the more important impact of BC on the albedo is less (or not) sensitive to the mixing state of the aerosols.

L226 : “we display” : where ?

Response: We substituted ‘display’ with ‘used’.

L292 : “a small portion of the emitted BC”. Please quantify it.

Response: We have quantified the portion that lifted up in this particular day (≈ 516 kg).

L334 : “due to the generally dry weather when the fires were burning”. It can be also ascribed to the fact that dry deposition mostly occurs in the quasi-laminar sublayer close to the surface. Aerosols are quickly deposited close to the sources before being injected at higher altitudes and being transported away from sources.

Response: Thanks for this comment. We have included it in the manuscript.

L365 : “the anthropogenic contribution is larger”. For the sake of clarity, the authors might write that the anthropogenic is relatively larger in Southern Greenland in contrast to Northern Greenland but remains lower than the biomass burning contribution.

Response: Comment was added to the manuscript.

L367 : “the BC concentrations that are calculated here for the studied fire period are relatively high compared to those reported previously”. I am not sure this is always true. The authors should also quote more recent studies, e.g. Polashenski et al. (2015), Legrand et al. (2016) or Thomas et al. (2017), who have reported higher events of biomass burning BC deposition over Greenland. If the BC deposited on snow/ice surfaces is much larger in those studies, it also suggests higher surface BC concentrations.

Response: We thank the reviewer for providing the references and have added them to the previous section. Please see Line 425-426 for Polashenski et al (2015) and Legrand et al. papers.

However, the Thomas et al. paper is using another unit (g/m^2) and without knowing the density of the samples no conversion to ng/g (units used in the present) can be applied.

L378 and L389 : “dosages”. Do you mean concentrations / mixing ratios ?

Response: They are dosages of concentrations. It is now explained in the last paragraph of section 3.3 and in the caption of the respective Figure.

L397-398 : BC particles are probably not the main contributors to AOD in this region for two reasons : the BC loadings are rather low in comparison to other aerosol compounds and the diameter of BC-containing particles is much smaller than the wave-length ($0.5 \mu\text{m}$). A better proxy of the temporal evolution of the integrated BC would be the absorbing AOD (AAOD), which is also often provided at AERONET stations. The AAOD/AOD would be also a good indicator of the contribution of BC to the total AOD (even if BC is not the only absorbing component). This should be shown on Fig. 5.

Response: The reviewer has a very good point here and we tried to retrieve AAOD data as he suggested.

Though in Kangerlussuaq and Thule no AAOD Level 2 data are available for July-September 2017, while in Narsarsuaq AAOD Level 2 data are available for 2 September 2017 (when the fires had been already extinguished).

In Andrews et al. (2017) paper is stated that “One obvious limitation of the AERONET inversion retrievals is that the uncertainty of the derived SSA becomes very large at low values of AOD (Dubovik et al., 2000). To minimize the effects of this uncertainty, the AERONET Level 2 data invalidate all absorption-related values if the AOD at wavelength 440 nm (AOD440) is below 0.4 (Dubovik et al., 2000, 2002; Holben et al., 2006).” In page 6043 of the same paper it is stated that “It should be noted that AERONET does not recommend the use of absorption-related parameters (e.g., SSA, AAOD and complex index of refraction) at AOD440 below 0.4.” In our case, except for the characteristic peak of AOD that is attributed to the N. American fires, all the other AOD values were below 0.4.

Sometimes researchers use AAOD LEV 1.5 data, but these get high uncertainty (see Andrews et al, 2017). In page 6051 of the Andrews et al. (2017) paper is also stated that “Using the sum-of-squares propagation of errors to calculate the uncertainty in AAOD for both high and low AAOD cases results in an AAOD uncertainty of approximately 0.015 for both high- and low-AOD cases ... An AAOD uncertainty value of 0.015 suggests an uncertainty of about 60% in AAOD for AOD440 > 0.5 and more than 140% uncertainty in AAOD for AOD440 < 0.2.”

Therefore, we do not think that these uncertain LEV1.5 AAOD measurements should be plotted instead of AOD here. However, if the reviewer or the editor disagree, we have retrieved them and we could use them in a next step. Besides, we only used AOD as an indicator for the presence of the plume, and for that purpose it should be sufficient.

L401-407 : How do the authors explain the significant AOD enhancement at the beginning of September observed at Narsarsuaq station ?

Response: As the reviewer can see, in the attached **Fig.R2** we present the biomass burning BC from GFAS (upper panel) in the beginning of September and the footprint emission sensitivity from the Narsarsuaq station (bottom panel) on September 3rd. We observe that the highest footprint emission sensitivity is located exactly at the place where GFAS emissions are the highest (Canada). Therefore, we have a clear indication that the increase that the reviewer mentioned is due to the Canadian wildfires.

L422 : “was not studied”. Does it mean that the transport of those North American fire plumes was not correctly captured by FLEXPART ? It is indeed impossible to see on Fig. 6d as the vertical scale is not appropriate.

Response: Here, we wanted to state that the existence of the N. American fires in the attenuated backscatter measurements that we get from CALIOP was not further studied. The study of the N. American fires is beyond the scope of this paper. We have used a better formulation in the manuscript now.

Sect. 4.2 : The authors should remind that they calculated only the forcing due to the Greenland fires, which is itself small compared to the North American or Eurasian fires. It should also be said explicitly that the calculated radiative forcing values does not include semi-direct nor indirect effects, which may be dominant here.

Response: We have rewritten the first part of the section to include the information requested by the referee.

L436 : “cloudless conditions”. I do not understand the purpose of this. It is only an ideal simulation, which is not commented in the paper afterwards. What does it bring to the discussion ?

Response: The IRF for cloudless conditions is compared against IRF including clouds in the subsequent lines. IRF for cloudless conditions was included, as they show the potential maximum effect of the forcing. The results presented show that the clouds reduce both the TOA and BOA IRF.

L440-442 : It is not clear if the given values refer to the total radiative forcing of BC. What are the relative contributions of the direct radiative forcing of BC and of the radiative forcing of BC deposited on snow surfaces ? The authors also give the values without any uncertainty, but a lot of assumptions have been done to retrieve the BC emissions, the BC size distribution, the BC optical properties. Each of those hypothesis would lead to a range of values of IRF.

Response: The given values refer to the total instantaneous radiative forcing, that is including both the effect of atmospheric BC and BC deposited on the snow. The latter dominates the IRF contributing between 85 to 99 % depending on BC amount. This has been clarified in the manuscript.

The composition of the BC from the fire is not known. Hence average BC optical properties were adopted. We have subsequently performed an uncertainty analysis using realistic variations in BC optical properties. This uncertainty analysis is included in the supplementary material and referred to in the manuscript.

We have also performed a sensitivity study and estimated the uncertainty of the BC deposition over Greenland due to the use of different size distribution of BC particles (see answer to previous comments).

L 442: “Fig 7c depicts the temporal behaviour...” Does it represent calculations in cloudy conditions ?

Response: It is the cloudy conditions that are shown. This information has been added both in the text and the figure caption. The temporal behaviour is shown in Fig 7d. This typo has been corrected as well.

L443-444 : I don't see how this information (blue line) can be useful. The location of the pixel where the maximum IRF is found likely varies with time. Besides the analysis of this figure is not done in text. I recommend to remove it.

Response: We have removed the blue line from the plot. The idea of plotting the TOA max IRF was to show that the single pixel maximum and area averaged RFs peak at different times. However, we agree with the reviewer that this information was perhaps not so useful.

L448-455 : If the authors want to be able to compare their results to global studies, as it is done here, they need to multiply the value of RF by the area of the simulation domain to obtain a forcing value in watts, and then divide it by the surface area of the Earth to obtain an equivalent global radiative effect in mW/m² that could be compared to results for global studies.

Response: The cited value from Skeie et al. (2011) is not a global value, but a value representative for the Greenland ice sheet (Fig 17 of Skeie et al., 2011). It is this value we are comparing against. The values from Myhre et al (2013) are included in order to give the reader a global value to compare against. This has been clarified in the text. It is clear that, on a global scale, the obtained RF values are negligible.

L453-455 : What about the impact of North American and Eurasian fires, whose plumes reach Greenland during the studied period ?

Response: These plumes are not the focus of the present study. Similar plumes have been studied before, so we don't think focusing on these plumes would provide a lot of new information beyond what has been published before. More technically, we only estimate the impact of these plumes using backward calculations, whereas RF calculations would require forward calculations. We think this is out of scope of the present paper.

What we have done, instead, is to calculate the impact of the N. American fires in the surface concentrations of BC over Greenland (see section 3.3). This proved that the BC concentrations from the N. American fires in August 2017 are more than 1 order of magnitude higher compared with those produced from the Greenland fires of August 2017 (see updated Figure 4).

L456-457 : What is the albedo reduction due to BC deposition that can be ascribed to Greenland fires / to fires outside Greenland / to anthropogenic sources ? If the goal of the paper is indeed to focus on the impact of the Greenland fires, quantifying this effect and comparing it to the relative contribution of the different sources would be really valuable for the paper. The authors should also compare their albedo reduction values to previous studies, e.g. Polashenski et al. (2015).

Response: We now compare our results to those of Polashenski et al. (2015) in section 4.2. The detailed study of the fires outside Greenland and from anthropogenic sources is beyond the scope of this paper. Notice that the albedo effects can't be done on the basis of the backward calculations done for the other sources and would require totally new forward simulations. However, giving the range of surface BC concentrations over Greenland (section 3.3 and Figure 4) is already enough to conclude that the event that we studied in the current paper has minor effects on the albedo or RF compared to BC from the N. American fires or from anthropogenic sources simply because of the different magnitude and duration of these fires.

Sect. 5 : The conclusions may be more quantitative.

For example : L478-479 : the ratio of BC deposition from the different sources can be given

Response: We have not quantified how big the deposition from anthropogenic and biomass burning sources is, and we have removed this sentence from the manuscript.

L481-483 : the AOD enhancement can be precised

Response: Corrected.

L488 : "albedo change due to the BC deposition". Which sources have been considered ?

Response: Corrected. It is the albedo change due to BC deposition from the Greenland fire of 2017.

L496-500 : Remove this purely speculative sentence. The opposite could also be said, given the findings of the paper.

Response: These lines state that "The very large fraction of the BC emissions deposited on the Greenland Ice Sheet (30% of the emissions) makes these fires very efficient climate forcers on a per unit emission basis. If the expected future warming of the Arctic (IPCC, 2013) produces more fires in Greenland in the future (Keegan et al., 2014), this

could indeed cause substantial albedo changes and thus contribute to accelerated melting of the Greenland Ice Sheet.”

We do not understand why this is speculative. A fraction of 30% deposition on the Greenland ice sheet is substantial, much higher than from any other source type and source region, so – on a per unit mass basis – the forcing due to albedo change is efficient, even if it is small overall. The second sentence can perhaps be considered somewhat speculative, but we have now reformulated it and, moreover, we support it with references. Furthermore, it is not presented as a conclusion, so it should be very clear to the reader to what extent this sentence is speculative. We nevertheless consider it important enough to keep it.

The choice of the figures kept in the manuscript is rather strange. Most useful figures relevant for the discussion have been displaced to the Supplementary Material. I recommend to move them to the main paper.

Response: We have moved the figure with the calculated dosages to the manuscript (Fig. 4), as the dosages are discussed more in the text. We have now placed back to the supplements (Fig. S5) the figure of the footprint emission sensitivities that are not the main focus of the paper. We are willing to put more figures in the manuscript in a next step, if the reviewer point into this direction. The only reason for using limited number of figures was that this paper was intended to be short.

Fig. 2a: Are those values averaged over the simulation domain ? over Greenland ? I had hard time to figure out how those values could be realistic. I think there is either a issue with the unit or a mistake in the calculation. Shouldn't it be ng/m³ or ng/kg instead of ug/m³ ? The total concentrations of BC in the domain should be calculated as the volume average of the grid cell concentrations, not the sum over all grid cells in the domain..

Response: We thank the reviewer for this comment that we have now corrected. We now present the average vertical concentrations over Greenland from the 2017 fires in pg/m³ in the updated Figure 2.

Fig 2b : Here again, there is an issue with the unit. The color bar indicates ug/m² (which is probably right), but the caption says ng/m². Which one is correct ?

Response: We also appreciate reviewer's help to correct this mistake. The error was in the legend and it has now been updated.

Fig. 4 : It is extremely difficult to see the colored grid cells and read their values. Please improve the quality of this figure.

Response: Quality of the figures has been set to 300 dpi. This should solve the problem.

Fig. 5 : Does the altitude represent agl or amsl ? The orography in Greenland is not flat.

Response: It is agl altitude and we now clarify it in the legend.

Fig 5 : Why do you keep the contribution of fires burning outside Greenland but exclude the BC contribution of anthropogenic sources ? According to Fig. 4, their contribution is absolutely not negligible and they might modify the time series of column-integrated BC in Greenland.

Response: We thank the reviewer for this comment. We tried to put also anthropogenic BC in these time-series. Column-integrated anthropogenic BC is very low and a stacked

line does not show anything in the time-series and that's the reason that we decided not to present it. We have added a small comment in the legend.

Fig. 6 : it would be better to use the same scale for longitude and altitude on panels (b) and (d).

Response: The reason that we did not use the same scale for longitude and altitude in these two figures is due to the small aerosol structure at high altitudes seen in the CALIOP data. We thought that this is likely due to the N. American fires that were burning at the same time with the Greenland ones. This is visible from the AOD measurements at many of the Greenland stations where large increases in AOD were observed.

In a previous comment for the AOD increase in the Narsarsuaq station at the beginning of September, we provided relevant footprint emission sensitivities and biomass burning emissions from CAMS_GFAS (see Figure R2). They explicitly show that the largest footprint was found in Canada in areas with large biomass burning emissions. However, since we do not study the impact of the N. American fires in detail, the sentences about the presence of N. American fire plumes at high altitudes in section 4.1 are rather speculative and we have removed them. We have also corrected Figure 6, as the reviewer suggested and for this, we acknowledge him.

Fig. 7c : Is the snow albedo reduction plotted for 31 August or for the full period ?

Response: The snow albedo reduction due to BC deposition from the beginning of the fires until 31 August is plotted in Figure 7c (please see last paragraph of section 4). Legend has also been updated.

Table 1 : This table is not commented nor analyzed in text. We can notice changes in the sources of RS data at different periods, which should be detailed in the methodology section.

Response: In line 105 we state that we used different RS data to better delineate fire perimeters and define burn severity. Which day each RS tool was used is shown by pointing to Table 1. In addition, discussion of the results presented in Table 1 is presented in section 3.1 and 3.2.

Legrand, M., et al. (2016), Boreal fire records in Northern Hemisphere ice cores: A review, *Clim. Past*, 12(10), 2033–2059.

Polashenski, C. M., J. E. Dibb, M. G. Flanner, J. Y. Chen, Z. R. Courville, A. M. Lai, J. J. Schauer, M. M. Shafer, and M. Bergin (2015), Neither dust nor black carbon causing apparent albedo decline in Greenland's dry snow zone: Implications for MODIS C5 surface reflectance, *Geophys. Res. Lett.*, 42, 9319–9327, doi:10.1002/2015GL065912.

Thomas, J. L., et al. (2017), Quantifying black carbon deposition over the Greenland ice sheet from forest fires in Canada, *Geophys. Res. Lett.*, 44, 7965–7974, doi:10.1002/2017GL073701.

Technical comments :

L350 : “adopted”. Do you mean “adapted” ?

Response: In this sentence we think that “adopted” fits better. We just used active fires from MODIS; we did not adapt anything.

L394 : Replace “for validating” by “to validate”.

Response: Corrected.

L485 : Replace “attenuation” by “attenuated”

Response: Corrected.

L512 : Please write “Brent Holben” in two words.

Response: Corrected.

REFERENCES

- Holben, B. N., Eck, T. F., Slutsker, I., Smirnov, A., Sinyuk, A., Schafer, J., Giles, D., and Dubovik O.: AERONET's Version 2.0 quality assurance criteria, http://aeronet.gsfc.nasa.gov/new_web/Documents/AERONETcriteria_final1.pdf, 2006.
- Andrews, E., Ogren, J. A., Kinne, S., and Samset, B.: Comparison of AOD, AAOD and column single scattering albedo from AERONET retrievals and in situ profiling measurements, *Atmos. Chem. Phys.*, 17, 6041-6072, <https://doi.org/10.5194/acp-17-6041-2017>, 2017.
- Dubovik, O., Smirnov, A., Holben, B. N., King, M. D., Kaufman, Y. J., Eck, T. F., and Slutsker, I.: Accuracy assessment of aerosol optical properties retrieval from AERONET sun and sky radiance measurements, *J. Geophys. Res.*, 105, 9791–9806, 2000.
- Paugam, R., Wooster, M., Atherton, J., Freitas, S. R., Schultz, M. G., and Kaiser, J. W.: Development and optimization of a wildfire plume rise model based on remote sensing data inputs – Part 2, *Atmos. Chem. Phys. Discuss.*, 15, 9815-9895, <https://doi.org/10.5194/acpd-15-9815-2015>, 2015.

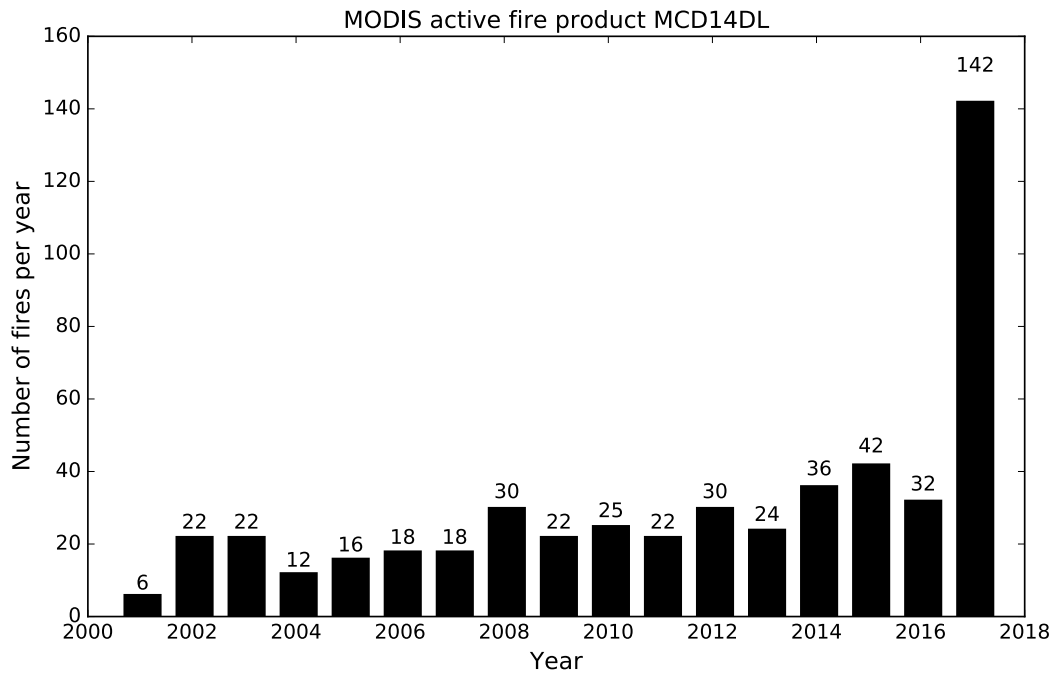


Fig. R 1. Annual number of active fires over Greenland during the last 17 years as seen from NASA's MODIS satellite (product MSC14DL).

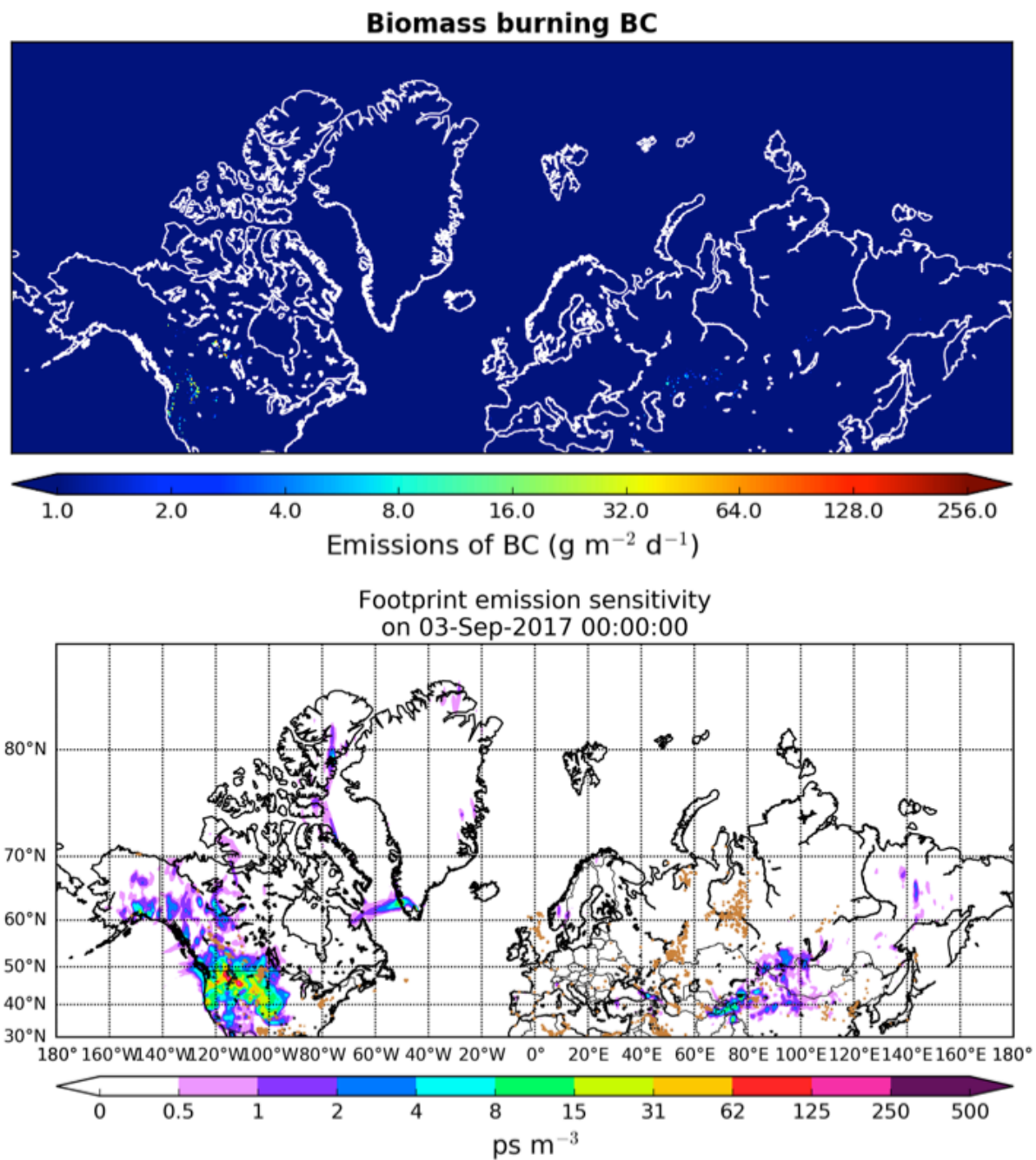


Fig. R 2. Biomass burning emissions of BC from GFAS (upper panel) in the beginning of September and the footprint emission sensitivity from the Narsarsuaq station (bottom panel) on September 3rd. The highest emission probability fits exactly to the place where the highest emissions occurred.

1 Open fires in Greenland in summer 2017: transport,
2 deposition and radiative effects of BC, OC and BrC
3 emissions,

4
5 **Nikolaos Evangeliou^{1,*}, Arve Kylling¹, Sabine Eckhardt¹, Viktor Myroniuk²,**
6 **Kerstin Stebel¹, Ronan Paugam³, Sergiy Zibtsev², Andreas Stohl¹**

7
8 ¹Norwegian Institute for Air Research (NILU), Department of Atmospheric and Climate
9 Research (ATMOS), Kjeller, Norway.

10 ²National University of Life and Environmental Sciences of Ukraine, Kiev, Ukraine.

11 ³King's College London, London, United Kingdom.

12
13 * Corresponding author: N. Evangeliou (Nikolaos.Evangeliou@nilu.no)
14

Nikolaos Evangeliou 25/5/2018 09:53

Deleted: Open fires in Greenland: an unusual event and its impact on the albedo of the Greenland Ice Sheet

Andreas Stohl 5/12/2018 12:35

Deleted: and impact on the Greenland Ice Sheet

20 **Abstract**

21 Highly unusual open fires burned in Western Greenland between 31 July and 21 August
22 2017, after a period of warm, dry and sunny weather. The fires burned on peat lands that
23 became vulnerable to fires by permafrost thawing. We used several satellite data sets to
24 estimate that the total area burned was about 2345 hectares. Based on assumptions of typical
25 burn depths and emission factors for peat fires, we estimate that the fires consumed a fuel
26 amount of about 117 kt C and emitted about 23.5 t of black carbon (BC), and 731 t of organic
27 carbon (OC) including 141 t of brown carbon (BrC). We used a Lagrangian particle
28 dispersion model to simulate the atmospheric transport and deposition of these species. We
29 find that the smoke plumes were often pushed towards the Greenland Ice Sheet by westerly
30 winds and thus a large fraction of the emissions (30%) was deposited on snow or ice covered
31 surfaces. The calculated deposition was small compared to the deposition from global
32 sources, but not entirely negligible. Analysis of aerosol optical depth data from three sites in
33 Western Greenland in August 2017 showed strong influence of forest fire plumes from
34 Canada, but little impact of the Greenland fires. Nevertheless, CALIOP lidar data showed that
35 our model captured the presence and structure of the plume from the Greenland fires. The
36 albedo changes and instantaneous surface radiative forcing in Greenland due to the fire
37 emissions were estimated with the SNICAR model and the uvspec model from the libRadtran
38 radiative transfer software package. We estimate that the maximum albedo change due to the
39 BC and BrC deposition was about 0.007, too small to be measured. The average instantaneous
40 surface radiative forcing over Greenland at noon on 31 August was 0.03–0.04 W m⁻², with
41 locally occurring maxima of 0.63–0.77 W m⁻² (depending on the studied scenario). The
42 average value is up to an order of magnitude smaller than the radiative forcing from other
43 sources. Overall, the fires burning in Greenland in summer of 2017 had little impact on the
44 Greenland Ice Sheet, causing a small extra radiative forcing. This was due to the – in a global
45 context – still rather small size of the fires. However, the very large fraction of the emissions
46 deposited on the Greenland Ice Sheet makes these fires very efficient climate forcers on a per
47 unit emission basis. If the expected future warming of the Arctic produces more severe fires
48 in Greenland, this could indeed cause albedo changes and thus contribute to accelerated
49 melting of the Greenland Ice Sheet. The fires burning in 2017 may be a harbinger of such
50 future events.

51

Nikolaos Evangeliou 4/12/2018 14:52
Deleted: BC ...mission factors for pe ... [1]

Andreas Stohl 5/12/2018 12:53
Deleted: ...and 731 t of organic carb ... [2]

Nikolaos Evangeliou 19/6/2018 15:29
Deleted: the

Andreas Stohl 5/12/2018 12:37
Deleted: BC

Nikolaos Evangeliou 4/12/2018 14:54
Deleted: BC ...missions (7 t or ...0% ... [3]

Andreas Stohl 16/6/2018 17:59
Deleted: very effectively

Nikolaos Evangeliou 4/12/2018 14:55
Deleted: BC ...missions were estima ... [4]

Andreas Stohl 16/6/2018 18:00
Deleted: by satellites or other means

Nikolaos Evangeliou 4/12/2018 14:57
Deleted: um values...of 0.63–0.77 W ... [5]

Andreas Stohl 16/6/2018 18:03
Deleted: changes

90 **1 Introduction**

91 In August 2017 public media reported unprecedented fire events in Western Greenland
92 (BBC News, 2017; New Scientist Magazine, 2017). These events were documented with
93 airborne photographs (SERMITSIAQ, 2017) and satellite images (NASA, 2017b) and raised
94 public concerns about the effects of climate change and possible impacts of soot emissions on
95 ice melting. Historically, wildfires have occurred infrequently on Greenland, because three-
96 quarters of the island is covered by a permanent ice sheet and permafrost is found on most of
97 the ice-free land (Abdalati and Steffen, 2001). Permafrost, or permanently frozen soil, lies
98 under a several meters thick “active” soil layer that thaws seasonally. But in certain areas,
99 where the permafrost layer starts melting, it can expose peat, a material consisting of only
100 partially decomposed vegetation that forms in wetlands over the course of hundreds of years
101 or longer. Peatlands, also known as bogs and moors, are the earliest stage in the formation of
102 coal. Globally, the amount of carbon stored in peat exceeds that stored in vegetation and is
103 similar in size to the current atmospheric carbon pool (Turetsky et al., 2014). When peatlands
104 dry, they are often affected by fires burning into the peat layers. Peat fires are difficult to
105 extinguish and they often burn until all the organic matter is consumed. Smoldering peat fires
106 already are the largest fires on Earth in terms of their carbon footprint (Turetsky et al., 2014).
107 For Greenland, it has been suggested that degradation of peat will accelerate towards 2080
108 (Daanen et al., 2011) and that the area affected by the fires in August 2017 is particularly
109 vulnerable to permafrost thawing (Daanen et al., 2011).

110 Fires in the high northern latitudes release significant amounts of CO₂, CH₄, N₂O, black
111 carbon (BC), and organic carbon (OC) and their emissions are often transported into Arctic
112 regions (Cofer III et al., 1991; Hao et al., 2016; Hao and Ward, 1993; Shi et al., 2015). While
113 BC is the most strongly light-absorbing component of the atmospheric aerosol (Bond et al.,
114 2013), a portion of OC compounds has shown strong absorption towards shorter wavelengths
115 of the electromagnetic spectrum (UV), therefore defined as brown carbon (BrC) (Andreae and
116 Gelencsér, 2006; Chakrabarty et al., 2010). BC is formed by the incomplete combustion of
117 fossil fuels, biofuels, and biomass (Bond et al., 2013). BrC is emitted from smoldering fires or
118 solid fuel combustion (Bond, 2001), from pyrolysis of biomass (Mukai and Ambe, 1986) and
119 from biogenic emissions of humic substances (Limbeck et al., 2003). Due to their particulate
120 nature, both BC and OC are important for human health (Lelieveld et al., 2015) and climate
121 impacts (Myhre et al., 2013). BC has an atmospheric lifetime of 3–11 days (Bond et al.,
122 2013), while BrC lifetimes are estimated at 5–7 days (Jo et al., 2016), thus facilitating

Andreas Stohl 16/6/2018 18:05
Deleted: s

Nikolaos Evangeliou 24/10/2018 12:47
Deleted: and

Nikolaos Evangeliou 24/10/2018 12:47
Deleted: ,

Nikolaos Evangeliou 24/10/2018 13:04
Deleted: and

Nikolaos Evangeliou 24/10/2018 13:48
Deleted: It is

Andreas Stohl 5/12/2018 12:41
Deleted: they

Andreas Stohl 5/12/2018 12:42
Deleted: all

Nikolaos Evangeliou 24/10/2018 13:49
Deleted: due to its

Nikolaos Evangeliou 24/10/2018 14:34
Deleted: ,

Andreas Stohl 5/12/2018 12:43
Deleted: presents

Nikolaos Evangeliou 24/10/2018 14:32
Deleted: and its

Nikolaos Evangeliou 24/10/2018 14:36
Deleted: es

135 transport over long distances (Forster et al., 2001; Stohl et al., 2006). BC, OC and BrC from
136 mid-latitude sources can thus reach remote areas such as the Arctic. They absorb solar
137 radiation in the atmosphere (Feng et al., 2013; Hansen and Nazarenko, 2004), have a
138 significant impact on cloud formation and also decrease surface albedo when deposited on ice
139 and snow and can accelerate melting processes (Hansen and Nazarenko, 2004; Wu et al.,
140 2016). This raises particular concerns about the effect of fires burning in the immediate
141 vicinity of the Greenland Ice Sheet. If a large fraction of the BC emitted by such fires is
142 deposited on the ice, these fires may be extremely effective in further enhancing the already
143 accelerating melting of the Greenland Ice Sheet (AMAP, 2017). BC, OC and BrC emissions
144 from such high latitude fires may also have a substantial effect on the albedo of sea ice.

145 Here we study transport and deposition of BC, OC and BrC over the Greenland Ice
146 Sheet from the fires that occurred in Western Greenland in August 2017, which likely
147 represent the largest fires that have occurred on Greenland in modern times (Figure S 1).
148 Since the fires occurred in an area entirely lacking ground-based observations, we use satellite
149 data and a Lagrangian atmospheric dispersion model for our study. Finally, we evaluate the
150 changes in the albedo of the Greenland Ice Sheet from the respective deposition of BC and
151 BrC and present instantaneous radiative forcing calculations for these two atmospheric
152 constituents released from the 2007 fires in Greenland.

153 2 Methods

154 2.1 Definition of burned area

155 Remote sensing has been useful for delineating fire perimeters, characterizing burn
156 severity and planning post-fire restoration activities in different regions. The use of satellite
157 imaging is particularly important for fire monitoring in remote areas due to difficult ground
158 access. The method that is presented in this section has been already used to calculate burned
159 area in the highly-contaminated radioactive forests of Chernobyl (Evangelou et al., 2014,
160 2015, 2016). Coordinates of fire locations (hot spots) were downloaded from FIRMS (Fire
161 Information for Resource Management System) (NASA, 2017a). For the mapping of the
162 burned area, Sentinel 2A images were used. To delineate fire perimeters and define burn
163 severity precisely, we used Landsat 8 Operational Land Imager (OLI) (resolution: 30×30 m)
164 together with Sentinel 1A (resolution: 30×30 m) and Sentinel 2A images (resolution: 30×30
165 m) (see Table 1) by applying the differenced Normalized Burn Ratio (dNBR) (Key and
166 Benson, 2006):

Nikolaos Evangeliou 24/10/2018 14:38

Deleted: BC

Nikolaos Evangeliou 24/10/2018 14:38

Deleted: s

Nikolaos Evangeliou 24/10/2018 14:39

Deleted: and has

Nikolaos Evangeliou 24/10/2018 14:39

Deleted: . It

Nikolaos Evangeliou 24/10/2018 14:39

Deleted: s

Andreas Stohl 16/6/2018 18:09

Deleted: probably

Nikolaos Evangeliou 23/5/2018 10:06

Deleted: of the Arctic

Nikolaos Evangeliou 5/12/2018 14:38

Deleted: Table 1

175
$$dNBR = NBR_{pre-fire} - NBR_{post-fire} \quad (\text{Eq. 1})$$

176 Normalized burn ratios for pre- ($NBR_{pre-fire}$) and postfire ($NBR_{post-fire}$) images from
177 Sentinel 2A can be calculated using radiances for near- and shortwave infrared bands (bands 8
178 (NIR) and 12 (SWIR2) at 0.835 μm and 2.202 μm , respectively):

179
$$NBR = \frac{1000 \cdot (NIR - SWIR2)}{NIR + SWIR2} \quad (\text{Eq. 2})$$

180 The methodology of applying a dNBR index to assess the impact of fires has been used in
181 forests of the Northern and Western USA (French et al., 2008; Key and Benson, 2006) and
182 elsewhere (Escuin et al., 2008; Sunderman and Weisberg, 2011).

183 The burned severity mosaics were created using Sentinel 2A images corrected for
184 atmospheric scattering (see Chavez, 1988). Pre- and post-fire images were used to create
185 cloudless mosaics for the area where the Greenland fires burned. A Maximum Value
186 Composite (MVC) procedure (Holben, 1986) was used to select pixels from each band that
187 were not cloud covered and have a high value of Normalized Difference Vegetation Index
188 (NDVI). To avoid spurious burn severity values, manually delineated fire perimeters were
189 applied and all areas outside were classified as unburned. We have used common dNBR
190 severity levels (Key and Benson, 2006) that are presented in [Figure 1](#). The occasionally dense
191 cloud cover was the main obstacle in reconstructing fire dynamics. As an independent source
192 of information, active fires from MODIS satellite product MCD14DL (Giglio et al., 2003) are
193 plotted in Supplemental Information (SI) [Figure S 2](#).

194 2.2 Injection altitudes, assumptions on biomass consumption and emissions 195 factors

196 Injection heights into the atmosphere of the emitted smoke were simulated with version
197 2 of the Plume Rise Model (PRM) (Paugam et al., 2015) which is implemented in the Global
198 Fire Assimilation System (GFAS) emission inventory (Rémy et al., 2017). The model
199 (hereafter referred to as PRMv2) is a further development of PRM (Freitas et al., 2006, 2010)
200 and has already been used in previous studies of fire events (Evangelou et al., 2015, 2016).
201 The model simulates a profile of smoke detrainment for every single fire, from which two
202 metrics are extracted: (i) a detrainment layer (i.e. where the detrainment rate is > 50% of its
203 global maximum) and (ii) an injection height (InjH, the top of the detrainment layer). Instead
204 of using the GFAS product, which uses the same statistics as in the PRMv2 InjH calculation,
205 we ran the model for every detected fire assuming a 6 h persistence and using the same
206 conversion factor as Kaiser et al. (2012) to estimate the biomass consumption. PRMv2 mass

Nikolaos Evangeliou 28/5/2018 14:03

Deleted: Additional classification rules were imposed t

Andreas Stohl 16/6/2018 23:00

Deleted: map burn severity more precisely

Nikolaos Evangeliou 28/5/2018 14:03

Deleted: due to the sensitivity of NBR to changes in vegetation and soil moisture. M

Nikolaos Evangeliou 5/12/2018 14:38

Deleted: Figure 1

Nikolaos Evangeliou 18/6/2018 09:31

Deleted: These confirm our results.

214 detrainment profiles are then time integrated and extracted at $1^{\circ} \times 1^{\circ}$ spatial resolution with a
 215 500 m vertical mesh to estimate the 3D distribution of biomass [burning smoke injection into](#)
 216 [the atmosphere](#). [Figure S 3](#), (SI) shows for all fires recorded in the MODIS fire product
 217 (Justice et al., 2002) during the fire period (31 July – 21 August 2017) the horizontal
 218 distribution of the median height of the emitted [smoke](#) and its integration over the longitude
 219 (right panel). Fires in Greenland showed a maximum injection height of around 2 km, but
 220 according to PRMv2 the majority of the emissions (90%) remained below 800 m. Low
 221 injection heights mostly inside the daytime planetary boundary layer are quite typical for
 222 smoldering fires including peat fires (Ferguson et al., 2003) such as those burning in
 223 Greenland (see below). For modeling the dispersion of [BC, OC and BrC](#) released from the
 224 Greenland fires, the emission profiles from PRMv2 were ingested into the Lagrangian particle
 225 dispersion model FLEXPART (see section 2.3).

226 Wildfires in boreal peatlands in the Canadian Arctic and in Alaska typically have
 227 (shallow) burn depths of 1–10 cm and consume 20–30 t C ha⁻¹ (Benscoter and Wieder, 2003;
 228 Shetler et al., 2008). [The consumed carbon](#) is often re-sequestered in 60–140 years after the
 229 fire (Turetsky et al., 2011; Wieder et al., 2009). Given that fire return intervals can be as short
 230 as 100–150 years in sub-humid continental peatlands (Wieder et al., 2009), and may exceed
 231 2000 years in humid climates (Lavoie and Pellerin, 2007), northern peatlands are generally
 232 resilient to wildfire (Magnan et al., 2012). For example, in peatlands of Northern Russia,
 233 organic matter available for combustion has been estimated to be 121.8 t C ha⁻¹ for forested
 234 lands and 21.3 t C ha⁻¹ for non-forested lands (Smirnov et al., 2015). Accordingly, a severe
 235 wildfire that burned within an afforested peatland in the Scottish Highlands during the
 236 summer of 2006 had a mean depth of burn of 17.5±2.0 cm (range: 1–54 cm) and a carbon loss
 237 of 96±15 t C ha⁻¹ (Davies et al., 2013). In contrast, tropical peatlands can have deep burn
 238 depths of 40–50 cm and release an average of 300–450 t C ha⁻¹ (Page et al., 2015; Reddy et
 239 al., 2015). In the present study, we assume an average amount of organic fuel available for
 240 combustion for the Greenland peat fires of August 2017 of 100 t C ha⁻¹, guided by values
 241 suggested [in Smirnov et al. \(2015\)](#).

242 [Estimation of the emissions of BC, OC and BrC, \$E_{BC,OC,BrC}\$ \(kg\), was based on the](#)
 243 following formula (Seiler and Crutzen, 1980; Urbanski et al., 2011) [using the calculated](#)
 244 [burned area \$A\$ \(ha\) and a number of assumptions:](#)

$$E_{BC,OC,BrC} = A \times FL \times \alpha \times EF \quad \text{Eq. 1}$$

Andreas Stohl 16/6/2018 23:06

Deleted: burned

Nikolaos Evangeliou 5/12/2018 14:38

Deleted: Figure S 3

Andreas Stohl 16/6/2018 23:07

Deleted: biomass

Andreas Stohl 16/6/2018 23:09

Deleted: , which

Nikolaos Evangeliou 24/10/2018 14:53

Deleted: elsewhere

Nikolaos Evangeliou 24/10/2018 14:53

Deleted: (

Nikolaos Evangeliou 24/10/2018 14:53

Deleted: .

Andreas Stohl 16/6/2018 23:11

Deleted: The

Andreas Stohl 16/6/2018 23:14

Deleted:

Nikolaos Evangeliou 24/10/2018 14:54

Deleted:

Andreas Stohl 16/6/2018 23:11

Deleted: from peat fires in Greenland were calculated fromus

Nikolaos Evangeliou 28/5/2018 14:04

Deleted: ing

259 | Here, FL is the mass of the fuel available for combustion (kg C ha^{-1}); α is the dimensionless
260 combustion completeness, which was adopted from Hao et al. (2016) for litter and duff fuels
261 (50%). EF is the emission factor (kg kg^{-1}), which was assumed to be 0.20 g kg^{-1} for BC and
262 6.23 g kg^{-1} for OC for peatland fires (Akagi et al., 2011). Emission factors for BrC are rarely
263 reported, as BrC is only a fraction of OC. To our knowledge, the only reported emission
264 factors in the literature for BrC are from forest fires in the United States (Aurell and Gullett,
265 2013) estimated to be $1.0\text{--}1.4 \text{ g kg}^{-1}$ (value used here: 1.2 g kg^{-1}). Fuel consumption is
266 calculated as the product of burned area, fuel loading and combustion completeness
267 ($A \times FL \times \alpha$).

268 2.3 Atmospheric modeling

269 | The emissions of BC, OC and BrC obtained from Eq. 1 were fed to the Lagrangian
270 particle dispersion model FLEXPART version 10.2 (Stohl et al., 2005) to simulate transport
271 and deposition. This model was originally developed for calculating the dispersion of
272 radioactive material from nuclear emergencies, but since then it has been used for many other
273 applications (e.g., Fang et al., 2014; Stohl et al., 2011, 2013). The model has a detailed
274 description of particle dispersion in the boundary layer and a convection scheme to simulate
275 particle transport in clouds (Forster et al., 2007). The model was driven by hourly $0.5^\circ \times 0.5^\circ$
276 operational analyses from the European Centre for Medium-Range Weather Forecasts
277 (ECMWF). Concentration and deposition fields were recorded in a global domain of $1^\circ \times 1^\circ$
278 spatial resolution with three hourly outputs. To capture the spatiotemporal variability of BC,
279 OC and BrC over the Greenland Ice Sheet, a nested domain with $0.05^\circ \times 0.05^\circ$ resolution was
280 used. The simulations accounted for wet and dry deposition, assuming a particle density of
281 1500 kg m^{-3} and a logarithmic size distribution with an aerodynamic mean diameter of
282 $0.25 \mu\text{m}$ and a standard deviation of 0.3 (Hu et al., 2018; Long et al., 2013). The wet
283 deposition scheme considers below-cloud and in-cloud scavenging separately based on cloud
284 liquid water and cloud ice content, precipitation rate and cloud depth from ECMWF, as
285 described in Grythe et al. (2017).

286 | To compare BC and OC concentrations in Greenland due to the emissions of the
287 Greenland fires to those due to emissions occurring elsewhere, we used the so-called
288 “retroplume” mode of FLEXPART for determining the influence of other sources. For only a
289 few receptor points, this mode is computationally more efficient than forward simulations.
290 Computational particles were tracked 30 days back in time from four receptor regions:
291 Northwestern (-62°E to -42°E , 72°N to 83°N), Southwestern (-62°E to -42°E , 61°N to 72°N),

Andreas Stohl 16/6/2018 23:14
Deleted: whereis the BC emission from the fire (kg); A is the burned area (ha);

Nikolaos Evangeliou 25/10/2018 10:50
Deleted: and

Nikolaos Evangeliou 24/10/2018 14:57
Deleted: o

Nikolaos Evangeliou 24/10/2018 14:57
Deleted: f

Nikolaos Evangeliou 24/10/2018 14:57
Deleted: (kg kg^{-1}) that was adopted from Akagi et al. (2011)

Nikolaos Evangeliou 24/10/2018 14:58
Deleted: ($0.0002 \text{ kg kg}^{-1}$)

Andreas Stohl 5/12/2018 12:56
Deleted: emissions

Andreas Stohl 5/12/2018 12:56
Deleted: ones

Nikolaos Evangeliou 25/10/2018 13:01
Deleted: BC

Andreas Stohl 16/6/2018 23:20
Deleted: In t

Andreas Stohl 16/6/2018 23:21
Deleted: , c

Andreas Stohl 16/6/2018 23:21
Deleted: a

Andreas Stohl 16/6/2018 23:21
Deleted: were tracked 30 days back in time. We used four receptor regions

308 Northeastern (-42°E to -17°E, 72°N to 83°N) and Southeastern Greenland (-42°E to -17°E,
309 61°N to 72°N). The retroplume mode allowed identification of the origin of BC and OC
310 through calculated footprint emission sensitivities (often also called source-receptor
311 relationships) that express the sensitivity of the BC and OC surface concentrations at the
312 receptor to emissions on the model output grid. If these emissions are known, BC and OC
313 concentrations at the receptor can be calculated as the product of the emission flux and the
314 emission sensitivity. Also, detailed source contribution maps can be calculated, showing
315 which regions contributed to the simulated concentration. For the anthropogenic emissions,
316 we used the ECLIPSE (Evaluating the CLimate and Air Quality ImPacts of ShortlivEd
317 Pollutants) version 5 (Klimont et al., 2017) emission data set. For the biomass burning
318 emissions outside Greenland, we used operational CAMS GFAS emissions (Kaiser et al.,
319 2012). To our knowledge, actual gridded emissions of BrC are not yet available.

320 2.4 Instantaneous radiative forcing (IRF) calculations

321 The IRF of the emitted substances of interest were calculated using the uvspec model
322 from the libRadtran radiative transfer software package (<http://www.libradtran.org/doku.php>)
323 (Emde et al., 2016; Mayer and Kylling, 2005). The radiative transfer equation was solved in
324 the independent pixel approximation using the DISORT model in pseudo-spherical geometry
325 with improved treatment of peaked phase functions (Buras et al., 2011; Dahlback and
326 Stamnes, 1991; Stamnes et al., 1988). Radiation absorption by gases was taken from the Kato
327 et al. (1999) parameterization modified as described in the libRadtran documentation and
328 Wandji Nyamsi et al. (2015). External mixture of aerosols was assumed, i.e. BC and BrC
329 were treated in isolation of other aerosol types that may also have been present in the plume.
330 This assumption likely leads to underestimates of the radiative impacts, at least for BC
331 (Jacobson, 2001), in the atmosphere as coating, for example, can enhance its radiative effects.
332 However, these assumptions should have little impact on the more important albedo
333 calculations (see below). For snow-covered surfaces, deposited BC and BrC were assumed to
334 reside in the uppermost 5 mm. Below 5 mm the snow was assumed to be without any
335 impurities. The albedo of the snow was calculated with the SNICAR model
336 (<http://snow.engin.umich.edu/info.html>) in a two-layer configuration (Flanner et al., 2007,
337 2009).

338 The IRF was calculated for three scenarios: (a) BC only, (b) BC and BrC and (c) BC and
339 BrC, where all OC is considered to be BrC. The BC only scenario demonstrates the impact of
340 BC alone, while the two other scenarios provide an estimate of the additional impact of BrC

Nikolaos Evangeliou 25/10/2018 13:02

Deleted: the

Nikolaos Evangeliou 28/5/2018 14:23

Deleted: global MODIS-satellite hot spot data (Giglio et al., 2003) and a simple emission scheme (Stohl et al., 2007), with emission factors for BC adopted from Andrea and Merlet (2001) and Akagi et al. (2011)

Andreas Stohl 5/12/2018 12:58

Deleted: RR

Nikolaos Evangeliou 3/12/2018 13:43

Deleted: radiative forcing (

Nikolaos Evangeliou 3/12/2018 13:43

Deleted:)

Nikolaos Evangeliou 25/10/2018 13:52

Deleted: BC

Nikolaos Evangeliou 25/10/2018 13:53

Deleted: was

Andreas Stohl 17/6/2018 14:42

Deleted: Liquid water and ice water clouds were adopted from ECMWF operational analysis data. No aerosols except those emitted from the Greenland fires were included. As such, the RF calculations represent a maximum estimate of the effect of BC from the Greenland fires.

Nikolaos Evangeliou 25/10/2018 13:22

Deleted: as

Nikolaos Evangeliou 25/10/2018 13:24

Deleted: of

Nikolaos Evangeliou 25/10/2018 13:25

Deleted: the

Nikolaos Evangeliou 25/10/2018 13:25

Deleted: of BC

Nikolaos Evangeliou 25/10/2018 13:53

Deleted: as

Andreas Stohl 5/12/2018 13:00

Deleted: and

365 in the plume, with the last scenario considered to be a maximum estimate. We calculated both
366 the bottom of the atmosphere (BOA) and top of atmosphere (TOA) instantaneous radiative
367 forcing (IRF) due to the Greenland fires at 1°×1° resolution. The IRF includes both the effects
368 of BC and BrC in the atmosphere, and deposited in snow. Note that the IRF does not include
369 any semi-direct nor indirect effects. We show IRF for cloudy conditions, which represents the
370 possible radiative effects of BC and BrC due to the 2017 fires with respect to the actual
371 meteorological situation. Liquid and ice water clouds were adopted from ECMWF.

372 2.5 Remote sensing of the smoke plume

373 To confirm the presence of the emitted substances from the Greenland fires and
374 elsewhere in the atmosphere over Greenland, we used the AERONET (AErosol RObotic
375 NETwork) data (Holben et al., 1998). AERONET provides globally distributed observations
376 of spectral aerosol optical depth (AOD), inversion products, and precipitable water in diverse
377 aerosol regimes. We chose data from three stations that were close to the 2017 fires and for
378 which cloud-free data exist for most of the simulated period, namely Kangerlussuaq
379 (50.62°W–66.99°N), Narsarsuaq (45.52°W–61.16°N) and Thule (68.77°W–76.51°N). Their
380 locations are shown in Figure S 2. We used Level 2.0 AOD data (fine and coarse mode AOD
381 at 500 nm and total AOD at 400 nm) from the AERONET version 3 direct-sun spectral
382 deconvolution algorithm (SDA version 4.1) product (downloaded on 20 July 2018) for the
383 simulated period (31 July to 31 August 2017).

384 To examine in particular the vertical depth of the smoke, we used data from the
385 CALIOP (Cloud-Aerosol Lidar with Orthogonal Polarization) lidar on the CALIPSO (Cloud-
386 Aerosol Lidar and Infrared Pathfinder Satellite Observations) platform (Winker et al., 2009).
387 CALIOP provides profiles of backscatter at 532 nm and 1064 nm, as well as the degree of the
388 linear polarization of the 532 nm signal. For altitudes below 8.3 km lidar profiles at 532 nm
389 are available with a vertical resolution of 30 m. We have utilized the level 1 data products
390 (version 3.40) of total attenuated backscatter at 532 nm. This signal responds to aerosols (like
391 BC, OC and BrC) as well as water and ice clouds, which in most cases can be distinguished
392 based on their differences in optical properties. The data were downloaded from the ICARE
393 Data and Services Center (<http://www.icare.univ-lille1.fr/>).

Andreas Stohl 17/6/2018 14:45

Deleted: ... [6]

Nikolaos Evangeliou 3/12/2018 14:02

Deleted: ic

Nikolaos Evangeliou 25/10/2018 13:26

Deleted: BC

Nikolaos Evangeliou 25/10/2018 13:26

Deleted: BC

Nikolaos Evangeliou 3/12/2018 14:02

Deleted: o

Nikolaos Evangeliou 3/12/2018 14:02

Deleted: the

Nikolaos Evangeliou 3/12/2018 14:03

Deleted: also calculated

Nikolaos Evangeliou 3/12/2018 14:04

Deleted: both cloudless and cloudy conditions. IRF for

Nikolaos Evangeliou 3/12/2018 14:04

Deleted: less

Nikolaos Evangeliou 3/12/2018 14:04

Deleted: indicates the maximum

Nikolaos Evangeliou 3/12/2018 14:05

Deleted: irrespective

Nikolaos Evangeliou 3/12/2018 14:05

Deleted: of

Nikolaos Evangeliou 3/12/2018 14:05

Deleted: , while IRF for cloudy conditions is representative of the actual conditions. For the latter, I

Nikolaos Evangeliou 25/10/2018 14:29

Deleted: BC

Nikolaos Evangeliou 25/10/2018 14:29

Deleted: fires in

Nikolaos Evangeliou 5/12/2018 14:38

Deleted: Figure S 2

Nikolaos Evangeliou 30/5/2018 15:47

Deleted: display

Nikolaos Evangeliou 21/6/2018 19:22

Deleted: at 00 nm

Nikolaos Evangeliou 21/6/2018 19:07

Deleted: 15

Nikolaos Evangeliou 3/12/2018 14:24

Deleted: /11/2017

Nikolaos Evangeliou 5/11/2018 13:28

Deleted: via ftp

419 **3 Results**

420 **3.1 Indications of early permafrost degradation and fuel availability**

421 Table 1, reports burned areas in August 2017 calculated for Greenland. In total, 2345
422 hectares burned between 31 July and 21 August 2017 (Figure 1). We estimate that about 117
423 kt of carbon were consumed by these fires. The area burned is not large compared to the
424 global area burned each year (464 million hectares), or the areas burned in boreal North
425 America (2.6 million hectares) or boreal Asia (9.8 million hectares) (Randerson et al., 2012),
426 but still highly unusual for Greenland.

427 It is not yet known how these fires started. Fires on carbon-rich soils can be initiated by
428 an external source, e.g. lightning, flaming wildfire and firebrand, or self-heating. The fires
429 burned relatively close to the town of Sisimut, so it is quite possible that humans started the
430 fires. Self-heating is another possibility as porous solid fuels can undergo spontaneous
431 exothermic reactions in oxidative atmospheres at low temperatures (Drysdale, 2011;
432 Restuccia et al., 2017b). This process starts by slow exothermic oxidation at ambient
433 temperature, causing a temperature increase, which is determined by the imbalance between
434 the rate of heat generation and the rate of heat losses (Drysdale, 2011). Fire initiated by self-
435 heating ignition is a well-known hazard for many natural materials (Fernandez Anez et al.,
436 2015; Restuccia et al., 2017a; Wu et al., 2015) and can also occur in natural soils (Restuccia
437 et al., 2017b). Southwestern Greenland was under anticyclonic influence during the last week
438 of July and according to the MODIS ESDIS worldview tool, direct sunshine occurred for
439 eight consecutive days before the fires started at the end of July 2017. It might be possible
440 that this long period of almost continuous insolation at these latitudes in July heated the soil
441 enough to self-ignite. In any case, the continuous sunshine had dried the soil, making it
442 susceptible to fire.

443 The fact that these fires were burning for about three weeks but spread relatively slowly
444 compared to above-ground vegetation fires indicates that the main fuel was probably peat.
445 The predominant vegetation in Western Greenland varies from carbon-rich *Salix glauca* low
446 shrubs (mean canopy height: 95 cm), mainly at low altitude south-facing slopes with deep
447 soils and ample moisture, to dwarf-shrubs and thermophilous graminoid vegetation (Arctic
448 steppe) at higher altitudes (Jedrzejek et al., 2013). In addition, the observed smoke was nearly
449 white, indicating damp fuel, such as freshly thawed permafrost, which produces smoke rich in
450 OC aerosol (Stockwell et al., 2016).

Nikolaos Evangeliou 5/12/2018 14:38
Deleted: Table 1
Nikolaos Evangeliou 23/5/2018 10:36
Deleted: over
Nikolaos Evangeliou 23/5/2018 10:36
Deleted: from GlobCover 2009 (Global Land Cover Map at 300 m resolution) (Arino et al., 2008)
Nikolaos Evangeliou 5/12/2018 14:38
Deleted: Figure 1
Nikolaos Evangeliou 5/11/2018 13:51
Deleted: of

Nikolaos Evangeliou 25/10/2018 15:19
Deleted: organic carbon (
Nikolaos Evangeliou 25/10/2018 15:19
Deleted:)
Nikolaos Evangeliou 25/10/2018 15:19
Deleted: Notice that while OC is not strongly absorbing, it may contain some absorbing brown carbon, which would add to the albedo reduction of snow by BC. On the other hand, BC emission factors are relatively low for peat fires (see Akagi et al., 2011).

466 Literally no fires should be expected in Greenland, since there is little available fuel as
467 it has been suggested by global models and validated by observations (Daanen et al., 2011;
468 Stendel et al., 2008); the only way to provide substantial amounts of fuel in Greenland is
469 permafrost degradation. However, it has been suggested that significant permafrost loss in
470 Greenland may occur only by the end of the 21st century (Daanen et al., 2011; Stendel et al.,
471 2008). The fires in 2017 might indicate that significant permafrost degradation has occurred
472 sooner than expected.

473 3.2 Transport and deposition of BC in Greenland

474 We estimate that about 23 t of BC, and 731 t of OC, including 141 t of BrC, were
475 released from the Greenland fires in August 2017 (Table 1). According to the FLEXPART
476 model simulations, these emissions were transported and deposited as shown in Figure 2. Due
477 to the low injection altitude of the releases within the boundary layer, transport was relatively
478 slow and thus the emitted substances initially remained quite close to their source. Slow
479 transport was also favored by mostly anticyclonic influence during the first half of August. It
480 seems that even though katabatic winds from the Greenland Ice Sheet occasionally
481 transported the plume westwards, most of the time the large-scale circulation pushed the
482 plume back towards Greenland (see SI animations). Consequently, a large fraction of the
483 emitted substances were deposited in Southwestern Greenland. On 3 August a small portion
484 of the emitted BC, OC and BrC (0.5 t, 16.1 t and 3.1 t, respectively) were lifted higher into
485 the atmosphere and were transported to the east and deposited in the middle of the Ice Sheet
486 over the course of the following two days (4 and 5 August). From 5 to 8 August, when the
487 fires were particularly intense, the emitted aerosols were transported to the south, where they
488 were deposited at the southern part of the Ice Sheet and close to the coastline. At the same
489 time, another branch of the plume was moving to the north depositing BC, OC and BrC over
490 Greenland's western coastline up to 80°N. Around 10 August, the plume circulated north- and
491 then eastwards in the northwestern sector of the anti-cyclone and the emitted aerosols were
492 deposited to the northern part of the Ice Sheet until 13 August. From around 16 August, a
493 cyclone approached from the northwest and the smoke was briefly transported directly
494 eastwards along the southern edge of the cyclone (see SI animations). Strong rain associated
495 with the cyclone's frontal system appears to have largely extinguished the fire by 17 or 18
496 August, although smaller patches may have continued smoldering for a few more days before
497 they also died out. The exact fire behavior after 16 August is difficult to determine because of

Nikolaos Evangeliou 25/10/2018 15:21

Deleted: .5

Andreas Stohl 5/12/2018 13:05

Deleted: ,

Andreas Stohl 5/12/2018 13:05

Deleted: and

Nikolaos Evangeliou 5/12/2018 14:38

Deleted: Table 1

Andreas Stohl 17/6/2018 00:12

Deleted: following the prevailing atmospheric circulation

Nikolaos Evangeliou 5/12/2018 14:38

Deleted: Figure 2

Nikolaos Evangeliou 3/12/2018 14:26

Deleted: most BC

Nikolaos Evangeliou 3/12/2018 14:26

Deleted: its emission

Nikolaos Evangeliou 3/12/2018 14:25

Deleted: BC was

Nikolaos Evangeliou 26/10/2018 09:24

Deleted: was

Nikolaos Evangeliou 26/10/2018 09:24

Deleted: was

Nikolaos Evangeliou 26/10/2018 09:25

Deleted: BC was

Nikolaos Evangeliou 26/10/2018 09:25

Deleted: most of it was

Andreas Stohl 17/6/2018 00:15

Deleted: , while a

Andreas Stohl 17/6/2018 00:15

Deleted: on

Nikolaos Evangeliou 26/10/2018 09:26

Deleted: BC was

515 frequent dense cloud cover. However, satellite imagery on 21 August shows no smoke
516 anymore in the area where the fires had burned.

517 The total deposition of BC, OC and BrC from the fires in Greenland was estimated to
518 be 9 t, 280 t and 54 t, respectively, or about 39% of the total emissions. About 7 t of BC, 218 t
519 of OC and 42 t of BrC were deposited on snow or ice covered surfaces, which is equivalent to
520 30% of the total emissions. Most of the rest was deposited in the Baffin Bay between
521 Greenland and Canada and in the Atlantic Ocean. With 30% of the emissions deposited on
522 snow or ice surfaces, Greenland fires may have a relatively large efficiency for causing
523 albedo changes on the Greenland Ice Sheet.

524 By comparison, the respective BC deposition on snow and ice surfaces over Greenland
525 from global emissions of BC (from ECLIPSEv5) was only 0.4% (39 kt) of the total emissions.
526 Even the total deposition of BC in the Arctic (>67°N) was only about 3% (215 kt). This
527 indicates the high relative potential of Greenland fires to pollute the cryosphere (on a per unit
528 emission basis), likely also giving them a particularly high radiative forcing efficiency.
529 Considering that the projected rise of Greenland temperatures is expected to result in further
530 degradation of the permafrost (Daanen et al., 2011) and, hence, likely resulting in more and
531 larger peat fires on Greenland, this constitutes a potentially important climate feedback which
532 could accelerate melting of the glaciers and ice sheet of Greenland and enhance Arctic
533 warming.

534 We also calculated the concentration of the deposited carbon aerosols in Greenland
535 snow (Figure 3) by taking the ratio of deposited quantities and the amount of water deposited
536 by rain or snowfall during the same time period (31 July to 31 August 2017). As expected,
537 snow concentrations show the same general patterns as the simulated deposition with the
538 highest concentrations obtained close to the source (western side of Greenland). High snow
539 concentrations were also computed in some regions of the Ice Sheet due to relatively intense
540 precipitation events. By contrast, dry deposition (example for BC) over the Ice Sheets was
541 low (Figure S 4). Dry deposition was responsible for a major fraction of the deposition only in
542 regions where the plume was transported during dry weather, and in most of these regions
543 total deposition was low. A notable exception is the region close to the fires, where dry
544 deposition was relatively important due to the generally dry weather when the fires were
545 burning. It can be also ascribed to the fact that dry deposition occurs in the quasi-laminar sub-
546 layer close to the surface. A fraction of the aerosols can be quickly deposited close to the
547 sources before they are transported to higher altitudes and away from the sources (Bellouin

Nikolaos Evangeliou 26/10/2018 10:23

Deleted: is shown in Figure 2b. About

Nikolaos Evangeliou 26/10/2018 10:25

Deleted: of the 23.5 t of BC from the Greenland fires in summer 2017 emitted (

Nikolaos Evangeliou 26/10/2018 10:25

Deleted:) were deposited over Greenland

Andreas Stohl 17/6/2018 00:17

Deleted: , which is about 39% of the fires' total emissions

Nikolaos Evangeliou 26/10/2018 10:27

Deleted: (30% of the total emissions)

Nikolaos Evangeliou 26/10/2018 10:00

Deleted: .

Nikolaos Evangeliou 26/10/2018 10:31

Deleted: BC

Nikolaos Evangeliou 5/12/2018 14:38

Deleted: Figure 3

Nikolaos Evangeliou 26/10/2018 10:32

Deleted: BC

Nikolaos Evangeliou 26/10/2018 10:32

Deleted: BC

Nikolaos Evangeliou 26/10/2018 10:32

Deleted: of BC

Nikolaos Evangeliou 26/10/2018 10:33

Deleted: BC in

Nikolaos Evangeliou 26/10/2018 10:34

Deleted: of

Andreas Stohl 17/6/2018 00:24

Deleted: mostly

Andreas Stohl 16/6/2018 11:02

Deleted: Aerosols are

Andreas Stohl 16/6/2018 11:03

Deleted: being

Nikolaos Evangeliou 26/10/2018 11:13

Deleted: the

Andreas Stohl 16/6/2018 11:02

Deleted: injected at

Andreas Stohl 16/6/2018 11:02

Deleted: being transported

569 and Haywood, 2014). The average calculated snow concentration of BC on the Ice Sheet was
570 estimated to be $<1 \text{ ng g}^{-1}$, but in some areas snow concentrations reached up to 3 ng g^{-1} . These
571 higher values are substantial considering that measured concentrations of BC in snow
572 typically range up to 16 ng g^{-1} in most of Greenland (Doherty et al., 2010) or from 1 – 17 ng
573 g^{-1} in summer 2012 and 3–43 ng g^{-1} in summer 2013 (Polashenski et al., 2015) and up to 15
574 ppb C (ng g^{-1}) during preindustrial times (from 1740 to 1870) on average (Legrand et al.,
575 2016). OC concentrations in snow were 2 ng g^{-1} (ppb C), on average, with local maxima of 10
576 ng g^{-1} . They are lower than those measured in snow over several places in Antarctica (23–928
577 ppb C) (Antony et al., 2011; Grannas et al., 2004; Legrand et al., 2013; Lyons et al., 2007), in
578 Greenland (400–580 ppb C) (Grannas et al., 2004) or in the Alps (70–304 ppb C) (Legrand et
579 al., 2013). Snow BrC was estimated to be even less; though, to our knowledge, no available
580 measurements exist in the relevant literature so far.

581 It has been reported that the size of rapidly coagulated aerosol particles produced by
582 different types of fires ranges between 0.1 to 10 μm , but more than 90% of the mass lies
583 between 0.1 and 1 μm (e.g., Conny and Slater, 2002; Long et al., 2013; Zhuravleva et al.,
584 2017 and many others). Therefore, we simulated the Greenland fires with an aerodynamic
585 mean diameter of 0.25 μm for BC, OC and BrC and a logarithmic standard deviation of 0.3
586 (see section 2.3), because all these substances have more or less the same lifetimes (Bond et
587 al., 2013; Jo et al., 2016; Lim et al., 2003). To examine the sensitivity of deposition in the
588 Greenland Ice Sheet from the Greenland fires of 2017 to the particle size distribution used in
589 the model, we simulated the same event for particles with aerodynamic mean diameters of
590 0.1, 0.25, 0.5, 1, 2, 4 and 8 μm and calculated the relative standard deviation of deposition
591 normalized against the aerodynamic mean diameter of 0.25 μm that was our basic
592 assumption. The results are shown in Figure S 5 for BC. The use of different size distributions
593 for the BC particles produced from the 2017 fires created a relative uncertainty on the
594 deposited mass of BC in the Greenland Ice Sheet, which ranges from 10%–30% in 86% of the
595 Sheet's surface to up to 50% in the rest of the Sheet's surface. As expected, the calculated
596 uncertainty is sensitive to the use of larger particles for BC; though BC particles larger than 1
597 μm are rather rare in peat fires (Hosseini et al., 2010; Leino et al., 2014).

598 3.3 Impact from other emissions in the Northern Hemisphere

599 In summertime 2017, intense wildfires were reported in British Columbia, Western
600 Canada (NASA, 2017c), and fires also burned at mid latitudes in Eurasia, as is typical during
601 spring and summer (Hao et al., 2016). Previous studies of wildfires have shown that the

Andreas Stohl 17/6/2018 00:26

Deleted: during

Andreas Stohl 17/6/2018 00:26

Deleted: produced

Nikolaos Evangeliou 26/10/2018 14:35

Deleted: BC

Andreas Stohl 17/6/2018 00:26

Deleted: to

Andreas Stohl 5/12/2018 13:09

Deleted: present

Nikolaos Evangeliou 5/12/2018 14:38

Deleted: Figure S

608 produced energy can be sufficient to loft smoke above the boundary layer by supercell
609 convection (Fromm et al., 2005) even up to stratospheric altitudes (Leung et al., 2007). As a
610 result, emitted aerosols can become subject to long-range transport over long distances
611 (Forster et al., 2001; Stohl et al., 2007). To examine the impact of these fires in Greenland,
612 average footprint emission sensitivities were calculated for four compartments of Greenland
613 (Northwestern, Southwestern, Northeastern and Southeastern Greenland) for the period 31
614 July to 31 August 2017 and the results are shown in [Figure S 6](#) together with the active fires
615 in the Northern Hemisphere from 10 July to 31 August 2017 adopted from the MODIS
616 satellite product (MCD14DL) (Giglio et al., 2003). As can be seen in Figure S 6, fires in
617 Alaska and in Western Canada might have affected BC, OC and BrC concentrations in
618 Greenland, as the corresponding emission sensitivities are the highest in North America. On
619 the contrary, emissions from fires in Eurasia seem to have affected Greenland less.

620 Using gridded emissions for BC and OC, the contribution of both biomass burning and
621 anthropogenic sources to surface concentrations in the four different regions over Greenland
622 (Northwestern, Northeastern, Southwestern and Southeastern Greenland, [Figure S 7](#)) was
623 calculated (see section 2.3). Fires affected the northern part of Greenland more than the
624 southern part with an average BC concentration of about 30 ng m⁻³, almost twice the
625 respective average for Southern Greenland (≈16 ng m⁻³). OC simulated concentrations were
626 much higher than those of BC with an average concentration of 945 ng m⁻³ in North
627 Greenland, while the respective concentrations in the southern part were about 490 ng m⁻³.
628 About one third of BC and OC originated from wildfires in Eurasia and the rest from North
629 America where the year 2017 appears to have been a particularly high fire year. The
630 anthropogenic contribution to surface concentrations of BC and OC over Greenland was
631 between 14% to 50% of the total contribution from all biomass burning sources ([Figure S 7](#)),
632 similar to what has been suggested previously for the Arctic in summer (Winiger et al., 2017).
633 The anthropogenic contribution is larger in Southern Greenland than in Northern Greenland,
634 due to the shorter distance from the main emission areas of North America and Western
635 Europe, but it remains much lower than the biomass burning contribution. The concentrations
636 of BC and OC that are calculated for the studied fire period (31 July to 31 August 2017) are
637 relatively high compared to those reported previously. For instance, von Schneidemesser et al.
638 (2009) observed an annual average BC concentration of 20 ng m⁻³ at Summit (Greenland) in
639 2006, while Massling et al. (2015) reported a summer average BC concentration of 11 ng m⁻³
640 at station Nord (Greenland) between May 2011 and August 2013. As regards to OC, average

Nikolaos Evangeliou 26/10/2018 14:48
Deleted: BC

Andreas Stohl 17/6/2018 00:45
Deleted: shown

Nikolaos Evangeliou 26/10/2018 14:50
Deleted: BC emitted

Nikolaos Evangeliou 26/10/2018 14:50
Deleted: s

Nikolaos Evangeliou 5/11/2018 14:58
Deleted: BC

Nikolaos Evangeliou 5/11/2018 15:36
Deleted: the

Nikolaos Evangeliou 5/11/2018 15:38
Deleted: BC

Nikolaos Evangeliou 5/11/2018 15:48
Deleted: only about

Nikolaos Evangeliou 31/5/2018 11:36
Deleted: In contrast to biomass burning, t

Andreas Stohl 17/6/2018 00:48
Deleted: ,

Andreas Stohl 17/6/2018 00:48
Deleted: contrast to

Nikolaos Evangeliou 5/11/2018 15:39
Deleted: BC

Nikolaos Evangeliou 5/11/2018 15:39
Deleted: here

654 concentrations of its water soluble part were measured in 2006 between 194 and 730 ng m⁻³ in
655 Summit, Greenland (Anderson et al., 2008) showing a large decreasing trend compared to
656 previous years (Dibb et al., 2002). We attribute this difference in the calculated concentrations
657 to more active fires during 2017 in Greenland than in previous years (see Figure S 1).

658 As an example of the importance of Northern Hemispheric biomass burning emissions
659 for the air over Greenland, we present time-series of surface BC concentrations in
660 Northwestern, Northeastern, Southwestern and Southeastern Greenland from the fires in
661 Greenland and from all the other wildfire emission sources occurring outside Greenland
662 (North Hemisphere) for the same period of time (Figure 4). The calculated dosages
663 (concentrations summed over a specific time period) for the same time period were also
664 computed. The fires in Greenland affected mainly its western part with concentrations that
665 reached up to 4.8 ng m⁻³ (Southwestern Greenland on 10 August) and 4.4 ng m⁻³
666 (Northwestern Greenland on 12 August), while BC concentrations in the eastern part
667 remained significantly lower (Figure 4). These concentrations are substantial considering that
668 the observed surface BC concentrations in Greenland in summer are usually below 20 ng m⁻³
669 (Massling et al., 2015). Surface BC due to wildfires occurring outside Greenland was also low
670 most of the time in the studied period (up to 10 ng m⁻³ at maximum) except for a large peak
671 between 19 and 23 August that mainly affected Northern Greenland (Figure 4). The
672 concentrations during this episodic peak were as high as 27 ng m⁻³. During the same period,
673 the contribution from anthropogenic emissions was also a few ng m⁻³ (Figure 4). BC dosages
674 for the simulation period (31 July – 10 August 2017) in Western Greenland due to the
675 Greenland fires were about one order of magnitude smaller than dosages from fires elsewhere
676 but of the same order of magnitude as BC originating from anthropogenic emissions.

677 4 Discussion

678 4.1 A validation attempt

679 There are few observations available that can be used to validate our model results. We
680 use the AERONET and CALIOP data for some qualitative comparisons. We present only BC
681 here, but similar plots can be generated for OC, considering that we used the same scavenging
682 coefficients as for BC to represent the similar lifetimes of BC and OC (Bond et al., 2013; Jo
683 et al., 2016; Lim et al., 2003). Contours of simulated vertical distribution of BC and column-
684 integrated simulated BC from fires inside and outside Greenland are plotted together with
685 time-series of measured AOD (fine and coarse mode AOD at 500 nm and total AOD at 400

Nikolaos Evangeliou 31/5/2018 11:39

Deleted: the study period

Nikolaos Evangeliou 31/5/2018 11:39

Deleted: other

Andreas Stohl 17/6/2018 00:49

Deleted: (see Figure S 1)

Nikolaos Evangeliou 5/11/2018 16:19

Deleted: To compare how

Nikolaos Evangeliou 5/11/2018 16:19

Deleted: t

Nikolaos Evangeliou 5/11/2018 16:19

Deleted: were

Nikolaos Evangeliou 5/12/2018 14:38

Deleted: Figure 4

Nikolaos Evangeliou 5/12/2018 14:38

Deleted: Figure 4

Nikolaos Evangeliou 5/12/2018 14:38

Deleted: Figure 4

Nikolaos Evangeliou 5/12/2018 14:38

Deleted: Figure 4

Nikolaos Evangeliou 1/6/2018 15:58

Deleted: for

Nikolaos Evangeliou 1/6/2018 15:58

Deleted: ing

Andreas Stohl 5/12/2018 13:12

Deleted: assum

Andreas Stohl 5/12/2018 13:13

Deleted: observed identical

Nikolaos Evangeliou 21/6/2018 19:21

Deleted: at a wavelength of

701 | [nm](#)) for the AERONET stations Kangerlussuaq, Narsarsuaq and Thule ([Figure 5](#)). It can be
 702 | seen that observed AOD variations were in very good agreement with the variation of
 703 | simulated column-integrated BC from fires outside Greenland (mainly in Canada), confirming
 704 | that the transport of these fire plumes was well captured by FLEXPART. Good examples are
 705 | the peaks at Kangerlussuaq on 24 August, at Narsarsuaq on 19 August and at Thule on 21
 706 | August ([Figure 5](#)) that are attributed to the Canadian fires. The simulated contribution of the
 707 | Greenland fires to simulated BC burdens was negligible by comparison, except at
 708 | Kangerlussuaq in the beginning of August when the Greenland fire emissions were the
 709 | highest. This station is less than 100 km away from where the fires burned, but not in the
 710 | main direction of the BC plume transport. It seems the period of simulated fire influence
 711 | corresponds to a small increase of the observed AOD values of up to 20% ([Figure 5](#)).

712 | To validate the smoke plume's vertical extent, we used the CALIOP data. These data
 713 | were only available from 5 August 2017 onward and frequent dense cloud cover inhibited
 714 | lidar observations [at](#) the altitudes below the clouds. High aerosol backscatter was only found
 715 | in the close vicinity of the fires. [Figure 6a](#) shows NASA's ESDIS view of the plume on 14
 716 | August 2017 at 6 UTC (available: [https://worldview.earthdata.nasa.gov/?p=geographic&l=MODIS_Aqua_CorrectedReflectance_TrueColor\(hidden\),MODIS_Terra_CorrectedReflectance_TrueColor,MODIS_Fires_Terra,MODIS_Fires_Aqua,Reference_Labels\(hidden\),Reference_Features,Coastlines&t=2017-08-14&z=3&v=-54.13349998138993,66.35888052399868,-50.32103113049877,69.08420005412792](https://worldview.earthdata.nasa.gov/?p=geographic&l=MODIS_Aqua_CorrectedReflectance_TrueColor(hidden),MODIS_Terra_CorrectedReflectance_TrueColor,MODIS_Fires_Terra,MODIS_Fires_Aqua,Reference_Labels(hidden),Reference_Features,Coastlines&t=2017-08-14&z=3&v=-54.13349998138993,66.35888052399868,-50.32103113049877,69.08420005412792)), where
 721 | a clear smoke signal was recorded. [A CALIOP overpass through the edge of the plume allows studying its vertical structure.](#) Increased attenuated backscatter is found below ~1.5 km above
 722 | sea level between 52°E and 51°E ([Figure 6b](#); black line denotes the orography). [Figure 6c](#)
 723 | (red line), [shows that](#) the CALIOP overpass transects directly the simulated plume of the
 724 | Greenland fires. Notice that the simulated plume also agrees very well with the smoke as seen
 725 | in NASA's ESDIS picture ([Figure 6a](#)). The vertical distribution of simulated BC as a function
 726 | of longitude is illustrated in [Figure 6d](#). It corresponds very well to the vertical distribution of
 727 | aerosols observed by CALIOP ([Figure 6b](#)). In particular, the smoke resides at altitudes below
 728 | 1.5 km and at exactly the same location both in the simulations and observations.

730 | 4.2 Instantaneous radiative forcing and albedo effects

731 | [BOA IRF due to \(a\) BC only, \(b\) BC and BrC and \(c\) BC and BrC when all OC was](#)
 732 | [assumed to be BrC \(extreme scenario\)](#) for noon on 31 August 2017 is depicted in [Figure 7a-c](#).
 733 | This day is shown because almost all [the aerosols](#) emitted by the fires, had been deposited,

Nikolaos Evangeliou 5/12/2018 14:38
 Deleted: Figure 5

Nikolaos Evangeliou 5/12/2018 14:38
 Deleted: Figure 5

Nikolaos Evangeliou 5/12/2018 14:38
 Deleted: Figure 5

Andreas Stohl 17/6/2018 01:06
 Deleted: in

Nikolaos Evangeliou 5/12/2018 14:38
 Deleted: Figure 6

Andreas Stohl 17/6/2018 01:10
 Deleted: The structure of the plume can be identified in the CALIOP curtain by its i

Andreas Stohl 17/6/2018 01:13
 Deleted: (black line denotes the orography of the area)

Nikolaos Evangeliou 20/6/2018 14:00
 Deleted: white line in

Nikolaos Evangeliou 5/12/2018 14:38
 Deleted: Figure 6

Nikolaos Evangeliou 20/6/2018 14:01
 Deleted: Another cloud of enhanced attenuated backscatter is evident at 4–5 km altitude between 50.5°E and 48.5°E. This mid-tropospheric plume was not studied but is likely due to aerosol transport from the North American fires. These large wildfires are eager to lift smoke at stratospheric altitudes a ... [7]

Nikolaos Evangeliou 5/12/2018 14:38
 Deleted: Figure 6

Nikolaos Evangeliou 5/12/2018 14:38
 Deleted: Figure 6

Nikolaos Evangeliou 5/12/2018 14:38
 Deleted: Figure 6

Nikolaos Evangeliou 5/12/2018 14:38
 Deleted: Figure 6

Andreas Stohl 17/6/2018 09:59
 Deleted: Effect on snow and ic... [8]

Nikolaos Evangeliou 4/12/2018 11:17
 Deleted: R

Andreas Stohl 17/6/2018 10:17
 Deleted: The bottom of the atmosphe... [9]

Nikolaos Evangeliou 6/6/2018 11:49
 Deleted: at the bottom of the atmosp... [10]

Nikolaos Evangeliou 5/12/2018 14:38
 Deleted: Figure 7

Nikolaos Evangeliou 3/12/2018 13:58
 Deleted: , both for cloudless (Fig. 7... [11]

Nikolaos Evangeliou 4/12/2018 11:21
 Deleted: BC

Andreas Stohl 5/12/2018 13:14
 Deleted: aerosols

Nikolaos Evangeliou 4/12/2018 11:21
 Deleted: before

786 thus giving a high IRF via albedo reduction due to snow contamination. The IRF is the largest
787 over ice close to the fire site and at locations where relatively large amounts of BC and BrC
788 were deposited. For BC only, the maximum BOA (TOA) IRF is 0.63 W m^{-2} (0.59 W m^{-2}),
789 and the average 0.03 W m^{-2} (0.03 W m^{-2}). Including BrC slightly increases the maximum
790 BOA (TOA) IRF to 0.65 W m^{-2} (0.61 W m^{-2}), while the change in the average IRF values is
791 negligible. For the extreme BrC scenario, the maximum BOA (TOA) IRF is 0.77 W m^{-2} (0.71
792 W m^{-2}) and the average 0.04 W m^{-2} (0.06 W m^{-2}). So, including BrC in our analysis increases
793 BOA IRF by only 20% even for the extreme scenario.

794 The IRF depends on the optical properties of the smoke from the fire, which are not
795 known. Hence, a sensitivity analysis was performed where the single scattering albedo (SSA)
796 was perturbed in contrast to a “medium case” (Figure S 8a) that was adopted from the
797 SNICAR model (Flanner et al., 2007, 2009) and has been used for the discussion in the
798 previous paragraph. To estimate the uncertainty due to the choice of BC optical properties,
799 additional calculations were made by scaling the SSA (red solid lines in Figure S 8a). The
800 choices of these scaled SSA values were based on the SSA reported for various modified
801 combustion efficiencies (MCE) by Pokhrel et al. (2016). Pokhrel et al. (2016) reported an
802 MCE of 0.9 for peat land. As such, our adopted SSA may be considered low (compare black
803 solid line and red line with upward triangles). Figure S 8b shows the IRF as BC is deposited
804 for the three cases. It suggests that the IRF ranges between 40% and 130% of our above-
805 assumed medium-case values for realistic variation of the aerosol optical properties.

806 Figure 7d depicts the temporal behaviour of the cloudy TOA IRF averaged over
807 Greenland (daily averages) for BC only (red line), for BC and BrC (blue line) and for BC and
808 BrC, when all OC is assumed to be BrC (black line, extreme case scenario). The daily
809 averaged IRF is seen to increase as the plume from the fires spreads out and starts to decline
810 after the fires were extinguished at the end of the month. The fact that the reduction towards
811 end of August is relatively slow is caused by the effect of the albedo reduction, which persists
812 until clean snow covers the polluted snow. Overall, albedo reduction dominates the total IRF
813 averaged over Greenland for the period of study contributing between 85% (in the beginning
814 of the study period) to 99% (at the end of the study period) and increasing in relative
815 importance with time as atmospheric BC and BrC are removed. The largest IRF differences
816 between the BC only case IRF and the two BC+BrC cases occur when there is still smoke in
817 the air and the lowest IRF differences occur after August 15th. This indicates that BrC is most
818 important for the IRF when it is airborne, even in the extreme scenario. However, for the

- Nikolaos Evangeliou 4/12/2018 11:29
Deleted: BC
- Nikolaos Evangeliou 4/12/2018 11:29
Deleted: of snow
- Andreas Stohl 17/6/2018 10:18
Deleted: The IRF includes both the effects of atmospheric BC and BC deposited on the snow. The latter dominates the IRF contributing between 85 to 99 % to the IRF depending on BC amount. Note that the IRF does not include any semi-direct nor indirect effects. Cloudless conditions were assumed in Figure 7a, while in Figure 7b water and ice water clouds were adopted from ECMWF.
- Nikolaos Evangeliou 4/12/2018 11:29
Deleted: For the cloudless conditions, t
- Andreas Stohl 17/6/2018 10:12
Deleted: around
- Andreas Stohl 5/12/2018 13:15
Deleted: with
- Nikolaos Evangeliou 4/12/2018 11:30
Deleted: s
- Nikolaos Evangeliou 4/12/2018 11:30
Deleted: The maximum IRF is 1.82 W m^{-2} , while the average for Greenland is 0.05 W m^{-2} . For t
- Andreas Stohl 5/12/2018 13:17
Deleted: T
- Nikolaos Evangeliou 4/12/2018 11:31
Deleted: including clouds the maximum BOA RF
- Andreas Stohl 5/12/2018 13:18
Deleted: to
- Nikolaos Evangeliou 6/6/2018 11:52
Deleted: For IRF at the top of the ... [12]
- Nikolaos Evangeliou 4/12/2018 13:37
Deleted: In addition the daily avera ... [13]
- Andreas Stohl 17/6/2018 11:26
Deleted: The blue line in Figure 7d ... [14]
- Nikolaos Evangeliou 4/12/2018 13:45
Deleted: is
- Andreas Stohl 5/12/2018 13:22
Deleted: u
- Andreas Stohl 5/12/2018 13:22
Deleted: with
- Andreas Stohl 5/12/2018 13:22
Deleted: IRF or with the BC+BrC II ... [15]
- Andreas Stohl 5/12/2018 13:23
Deleted: are observed
- Andreas Stohl 5/12/2018 13:23
Deleted: e
- Andreas Stohl 5/12/2018 13:24
Deleted: ly
- Andreas Stohl 5/12/2018 13:24
Deleted: most

861 latter, the impact is also large after August 15th due to a further albedo decrease of about
862 0.001 compared to the case where only BC was considered.

863 According to Hansen et al. (2005) the TOA IRF of BC approximates the adjusted RF as
864 reported by Myhre et al. (2013). In their Table 8.4, Myhre et al. (2013) estimated the global
865 averaged RF due to BC between the years 1750 and 2011 to be +0.40 (+0.05 to +0.80) W m⁻².
866 Skeie et al. (2011) estimated a global mean radiative forcing of 0.35 W m⁻² due to fossil fuel
867 and biofuel increases between 1750 and 2000. For Greenland, Skeie et al. (2011) found the
868 RF to be less than about 0.2 W m⁻². This number may be compared to our area averaged IRF
869 estimate due to the Greenland fire. For cloudy conditions the TOA IRF over Greenland due to
870 the Greenland fires is about a factor 4 to 10 smaller compared with the RF over Greenland
871 due to BC from all global anthropogenic sources reported in Skeie et al. (2011).

872 The albedo reduction at 550 nm for the three scenarios (BC only, BC+BrC and BC+BrC
873 extreme) is shown in Figure 7e-g. The maximum albedo change is about 0.006 when only BC
874 was considered. Adding BrC from the most extreme scenario, the maximum albedo change
875 was calculated as 0.007. This albedo change has an impact on IRF, but it is too small to be
876 measured by satellites. For example, MODIS albedo estimates have been compared to in situ
877 albedo measurements in Greenland by Stroeve et al. (2005). They found that the root mean
878 square error between MODIS and in situ albedo values was ±0.04 for high quality flagged
879 MODIS albedo retrievals. Unmanned Aerial Vehicle (UAV) measurements over Greenland
880 made by Burkhart et al. (2017) have uncertainties of similar magnitude. Also, Polashenski et
881 al. (2015) reported that the albedo reduction due to aerosol impurities on the Greenland Ice
882 Sheet in 2012–2014 period is relatively small (mean 0.003), though episodic aerosol
883 deposition events can reduce albedo by 0.01–0.02. The albedo changes due to BC and BrC
884 from the Greenland fires are generally an order of magnitude smaller (Figure 7e-g) and thus
885 too small to be detected by present UAV and satellite instruments and retrieval methods
886 (Warren, 2013).

887 5 Conclusions

888 We studied atmospheric transport, deposition and impact of BC, BrC and OC emitted as
889 a result of unusual open fires burning in Greenland between 31 July and 21 August 2017. Our
890 conclusions can be summarized below:

- 891 • The fires burned on peat lands that became vulnerable by permafrost thawing. The region
892 where the fires burned was identified previously as being susceptible to permafrost

Nikolaos Evangeliou 6/6/2018 14:49

Deleted: calculated

Nikolaos Evangeliou 6/6/2018 14:50

Deleted: due to BC originating from fossil fuel and biofuel combustion relative to preindustrial times (1750)

Nikolaos Evangeliou 6/6/2018 14:51

Deleted: Thus, the calculated RF due to the Greenland fires f

Nikolaos Evangeliou 4/12/2018 13:55

Deleted: one order of magnitude

Nikolaos Evangeliou 18/6/2018 13:27

Deleted: (

Nikolaos Evangeliou 18/6/2018 13:27

Deleted: ,

Nikolaos Evangeliou 4/12/2018 13:57

Deleted: due to the deposited BC

Nikolaos Evangeliou 5/12/2018 14:38

Deleted: Figure 7Figure 7

Nikolaos Evangeliou 4/12/2018 13:57

Deleted: c

Andreas Stohl 17/6/2018 11:32

Deleted: the radiative forcing

Nikolaos Evangeliou 5/12/2018 14:38

Deleted: Figure 7Figure 7

Nikolaos Evangeliou 4/12/2018 14:01

Deleted: c

Nikolaos Evangeliou 4/12/2018 14:29

Deleted: The conclusions from our

Nikolaos Evangeliou 4/12/2018 14:29

Deleted: y of

Nikolaos Evangeliou 4/12/2018 14:30

Deleted: the

Nikolaos Evangeliou 4/12/2018 14:31

Deleted: are the following

912 melting; however, large-scale melting was expected to occur only towards the end of the
913 21st century. The 2017 fires show that at least in some locations substantial permafrost
914 thawing is already occurring now.

915 • The total area burned was about 2345 hectares. We estimate that the fires consumed a fuel
916 amount of about 117 kt C and emitted about 23.5 t of BC, and 731 t of OC, including 141 t
917 of BrC.

918 • The Greenland fires were small compared to fires burning at the same time in North
919 America and Eurasia, but a large fraction of BC, OC and BrC emissions (30%) was
920 deposited on the Greenland Ice Sheet.

921 • Measurements of aerosol optical depth at three sites in Western Greenland in August 2017
922 were strongly influenced by forest fires in Canada burning at the same time, but the
923 Greenland fires had an observable impact doubling the column-integrated BC
924 concentrations at the closest station.

925 • A comparison of the simulated BC releases in FLEXPART with the vertical cross-section
926 of total attenuated backscatter (at 532 nm) from CALIOP lidar showed that the
927 spatiotemporal evolution and particularly the top height of the plume was captured by the
928 model.

929 • We estimate that the maximum albedo change due to the BC deposition from the
930 Greenland fires was about 0.006, whereas adding deposited BrC increases albedo to 0.007
931 at maximum, which is too small to be measured. The average instantaneous BOA radiative
932 forcing over Greenland at noon on 31 August was between 0.03–0.04 W m⁻² for the three
933 scenarios (BC only, BC+BrC and BC+BrC extreme), with locally occurring maxima of
934 0.63 W m⁻², 0.65 W m⁻² and 0.77 W m⁻², respectively. The average value when only BC
935 was considered is up to an order of magnitude smaller than the radiative forcing due to BC
936 from other sources.

937 • We conclude that the fires burning in Greenland in summer of 2017 had small impact on
938 on the Greenland Ice Sheet, causing almost negligible extra radiative forcing. This was
939 due to the – in a global context – still rather small size of the fires.

940 The very large fraction of the emissions deposited on the Greenland Ice Sheet (30% of
941 the emissions) makes these fires very efficient climate forcers on a per unit emission basis.

942 Thus, while the fires in 2017 were still relatively small on a global scale, if the expected future
943 warming of the Arctic (IPCC, 2013) produces more and larger fires in Greenland (Keegan et

- Nikolaos Evangeliou 4/12/2018 14:33
Deleted: produced
- Nikolaos Evangeliou 4/12/2018 14:33
Deleted: BC emissions of
- Andreas Stohl 5/12/2018 13:25
Deleted: ,
- Andreas Stohl 5/12/2018 13:25
Deleted: and
- Nikolaos Evangeliou 5/11/2018 16:33
Deleted: their
- Nikolaos Evangeliou 4/12/2018 14:34
Deleted: or glaciers
- Nikolaos Evangeliou 4/12/2018 14:34
Deleted: This BC deposition was small compared to BC deposition from global anthropogenic and biomass burning sources, but not entirely negligible.
- Nikolaos Evangeliou 1/6/2018 15:59
Deleted: ion
- Andreas Stohl 5/12/2018 13:26
Deleted: by satellites or other means
- Andreas Stohl 17/6/2018 11:37
Deleted: surface
- Nikolaos Evangeliou 4/12/2018 14:43
Deleted: um values
- Nikolaos Evangeliou 4/12/2018 14:43
Deleted: .
- Nikolaos Evangeliou 4/12/2018 14:47
Deleted:
- Nikolaos Evangeliou 4/12/2018 14:47
Deleted: at least
- Nikolaos Evangeliou 4/12/2018 14:49
Deleted: little
- Nikolaos Evangeliou 4/12/2018 14:49
Deleted: BC deposition
- Nikolaos Evangeliou 4/12/2018 14:50
Deleted: BC
- Andreas Stohl 17/6/2018 11:39
Deleted: If
- Nikolaos Evangeliou 25/5/2018 12:30
Deleted: further
- Nikolaos Evangeliou 25/5/2018 12:30
Deleted: Greenland
- Nikolaos Evangeliou 25/5/2018 15:21
Deleted: much larger
- Nikolaos Evangeliou 4/12/2018 14:50
Deleted: in the future

969 | al., 2014), this could indeed cause substantial albedo changes and thus ~~contribute~~ to
970 accelerated melting of the Greenland Ice Sheet.

971

972 *Data availability.* All data used for the present publication can be obtained from the
973 corresponding author upon request.

974

975 *Competing financial interests.* The authors declare no competing financial interests.

976

977 *Acknowledgements.* This study was partly supported by the Arctic Monitoring and
978 Assessment Programme (AMAP) and was conducted as part of the Nordic Centre of
979 Excellence eSTICC (Nordforsk 57001). We acknowledge the use of imagery from the NASA
980 Worldview application (<https://worldview.earthdata.nasa.gov/>) operated by the
981 NASA/Goddard Space Flight Center Earth Science Data and Information System (ESDIS)
982 project. We thank Brent Holben and local site managers for their effort in establishing and
983 maintaining the AERONET sites used in this investigation. We thank NASA/CNES engineers
984 and scientists for making CALIOP data available. The lidar data were downloaded from the
985 ICARE Data and Service Center.

986

987 *Author contributions.* NE performed the simulations, analyses, wrote and coordinated the
988 paper. AK performed the radiation calculations and wrote parts of the paper. VM and SZ
989 performed GIS analysis for the burned area calculations. RP made all the runs for the
990 injection height calculations using the PRMv2 model. KS analysed satellite data for AOD and
991 CALIOP, SE and AS commented and coordinated the manuscript. All authors contributed to
992 the final version of the manuscript.

993

994 **References**

- 995 Abdalati, W. and Steffen, K.: Greenland Ice Sheet melt extent:1979-1999, *J. Geophys. Res.*
996 *Atmos.*, 106(D24), 33983–33988, doi:10.1029/2001JD900181, 2001.
- 997 Akagi, S. K., Yokelson, R. J., Wiedinmyer, C., Alvarado, M. J., Reid, J. S., Karl, T., Crounse, J.
998 D. and Wennberg, P. O.: Emission factors for open and domestic biomass burning for use
999 in atmospheric models, *Atmos. Chem. Phys.*, 11(9), 4039–4072, doi:10.5194/acp-11-
1000 4039-2011, 2011.
- 1001 AMAP: Snow, Water, Ice and Permafrost. Summary for Policy-makers, Arctic Monitoring
1002 and Assessment Programme (AMAP), Oslo, Norway. [online] Available from:
1003 [https://www.amap.no/documents/doc/Snow-Water-Ice-and-Permafrost.-Summary-](https://www.amap.no/documents/doc/Snow-Water-Ice-and-Permafrost.-Summary-for-Policy-makers/1532)
1004 [for-Policy-makers/1532](https://www.amap.no/documents/doc/Snow-Water-Ice-and-Permafrost.-Summary-for-Policy-makers/1532) (Accessed 27 November 2017), 2017.
- 1005 Anderson, C. H., Dibb, J. E., Griffin, R. J., Hagler, G. S. W. and Bergin, M. H.: Atmospheric
1006 water-soluble organic carbon measurements at Summit, Greenland, *Atmos. Environ.*,

Nikolaos Evangeliou 6/6/2018 15:23

Deleted: lead

1008 42(22), 5612–5621, doi:10.1016/j.atmosenv.2008.03.006, 2008.
1009 Andreae, M. O. and Gelencsér, A.: Black carbon or brown carbon? The nature of light-
1010 absorbing carbonaceous aerosols, *Atmos. Chem. Phys.*, 6(3), 3419–3463,
1011 doi:10.5194/acpd-6-3419-2006, 2006.
1012 Antony, R., Mahalinganathan, K., Thamban, M. and Nair, S.: Organic carbon in antarctic
1013 snow: Spatial trends and possible sources, *Environ. Sci. Technol.*, 45(23), 9944–9950,
1014 doi:10.1021/es203512t, 2011.
1015 Aurell, J. and Gullett, B. K.: Emission factors from aerial and ground measurements of
1016 field and laboratory forest burns in the southeastern U.S.: PM_{2.5}, black and brown
1017 carbon, VOC, and PCDD/PCDF, *Environ. Sci. Technol.*, 47(15), 8443–8452,
1018 doi:10.1021/es402101k, 2013.
1019 BBC News: “Unusual” Greenland wildfires linked to peat, [online] Available from:
1020 <http://www.bbc.com/news/science-environment-40877099> (Accessed 6 September
1021 2017), 2017.
1022 Bellouin, N. and Haywood, J.: *Aerosols: Climatology of Tropospheric Aerosols*, Second
1023 Edi., Elsevier., 2014.
1024 Benscoter, B. W. and Wieder, R. K.: Variability in organic matter lost by combustion in a
1025 boreal bog during the 2001 Chisholm fire, *Can. J. For. Res.*, 33(12), 2509–2513,
1026 doi:10.1139/x03-162, 2003.
1027 Bond, T. C.: Spectral dependence of visible light absorption by carbonaceous particles
1028 emitted from coal combustion, *Geophys. Res. Lett.*, 21(21), 4075–4078,
1029 doi:10.1029/2001GL013652, 2001.
1030 Bond, T. C., Doherty, S. J., Fahey, D. W., Forster, P. M., Berntsen, T., Deangelo, B. J., Flanner,
1031 M. G., Ghan, S., Kärcher, B., Koch, D., Kinne, S., Kondo, Y., Quinn, P. K., Sarofim, M. C.,
1032 Schultz, M. G., Schulz, M., Venkataraman, C., Zhang, H., Zhang, S., Bellouin, N., Guttikunda,
1033 S. K., Hopke, P. K., Jacobson, M. Z., Kaiser, J. W., Klimont, Z., Lohmann, U., Schwarz, J. P.,
1034 Shindell, D., Storelvmo, T., Warren, S. G. and Zender, C. S.: Bounding the role of black
1035 carbon in the climate system: A scientific assessment, *J. Geophys. Res. Atmos.*, 118(11),
1036 5380–5552, doi:10.1002/jgrd.50171, 2013.
1037 Buras, R., Dowling, T. and Emde, C.: New secondary-scattering correction in DISORT with
1038 increased efficiency for forward scattering, *J. Quant. Spectrosc. Radiat. Transf.*, 112(12),
1039 2028–2034, doi:10.1016/j.jqsrt.2011.03.019, 2011.
1040 Chakrabarty, R. K., Moosmüller, H., Chen, L. W. A., Lewis, K., Arnott, W. P., Mazzoleni, C.,
1041 Dubey, M. K., Wold, C. E., Hao, W. M. and Kreidenweis, S. M.: Brown carbon in tar balls
1042 from smoldering biomass combustion, *Atmos. Chem. Phys.*, 10(13), 6363–6370,
1043 doi:10.5194/acp-10-6363-2010, 2010.
1044 Chavez, P. S.: An improved dark-object subtraction technique for atmospheric scattering
1045 correction of multispectral data, *Remote Sens. Environ.*, 24(3), 459–479,
1046 doi:10.1016/0034-4257(88)90019-3, 1988.
1047 Cofer III, W. R., Levine, J. S., Winstead, E. L. and Stocks, B. J.: New estimates of nitrous
1048 oxide emissions from biomass burning, *Nature*, 349(6311), 689–691 [online] Available
1049 from: <http://dx.doi.org/10.1038/349689a0>, 1991.
1050 Conny, J. and Slater, J.: Black carbon and organic carbon in aerosol particles from crown
1051 fires in the Canadian boreal forest, *J. Geophys. Res.* ... [online] Available from:
1052 <http://onlinelibrary.wiley.com/doi/10.1029/2001JD001528/full>, 2002.
1053 Daanen, R. P., Ingeman-Nielsen, T., Marchenko, S. S., Romanovsky, V. E., Foged, N.,
1054 Stendel, M., Christensen, J. H. and Hornbech Svendsen, K.: Permafrost degradation risk
1055 zone assessment using simulation models, *Cryosphere*, 5(4), 1043–1056,
1056 doi:10.5194/tc-5-1043-2011, 2011.

1057 Dahlback, A. and Stamnes, K.: A new spherical model for computing the radiation field
1058 available for photolysis and heating at twilight, *Planet. Space Sci.*, 39(5), 671–683,
1059 doi:10.1016/0032-0633(91)90061-E, 1991.
1060 Davies, G. M., Gray, A., Rein, G. and Legg, C. J.: Peat consumption and carbon loss due to
1061 smouldering wildfire in a temperate peatland, *For. Ecol. Manage.*, 308, 169–177,
1062 doi:10.1016/j.foreco.2013.07.051, 2013.
1063 Dibb, J. E., Arsenault, M., Peterson, M. C. and Honrath, R. E.: Fast nitrogen oxide
1064 photochemistry in Summit, Greenland snow, *Atmos. Environ.*, 36(15–16), 2501–2511,
1065 doi:10.1016/S1352-2310(02)00130-9, 2002.
1066 Doherty, S. J., Warren, S. G., Grenfell, T. C., Clarke, A. D. and Brandt, R. E.: Light-absorbing
1067 impurities in Arctic snow, *Atmos. Chem. Phys.*, 10(23), 11647–11680, doi:10.5194/acp-
1068 10-11647-2010, 2010.
1069 Drysdale, D.: *An Introduction to Fire Dynamics*, 3rd Editio., John Wiley & Sons, Ltd.,
1070 2011.
1071 Emde, C., Buras-Schnell, R., Kylling, A., Mayer, B., Gasteiger, J., Hamann, U., Kylling, J.,
1072 Richter, B., Pause, C., Dowling, T. and Bugliaro, L.: The libRadtran software package for
1073 radiative transfer calculations (version 2.0.1), *Geosci. Model Dev.*, 9(5), 1647–1672,
1074 doi:10.5194/gmd-9-1647-2016, 2016.
1075 Escuin, S., Navarro, R. and Fernández, P.: Fire severity assessment by using NBR
1076 (Normalized Burn Ratio) and NDVI (Normalized Difference Vegetation Index) derived
1077 from LANDSAT TM/ETM images, *Int. J. Remote Sens.*, 29(4), 1053–1073,
1078 doi:10.1080/01431160701281072, 2008.
1079 Evangeliou, N., Balkanski, Y., Cozic, A., Hao, W. M. and Møller, A. P.: Wildfires in
1080 Chernobyl-contaminated forests and risks to the population and the environment: A
1081 new nuclear disaster about to happen?, *Environ. Int.*, 73, 346–358,
1082 doi:10.1016/j.envint.2014.08.012, 2014.
1083 Evangeliou, N., Balkanski, Y., Cozic, A., Hao, W. M., Mouillot, F., Thonicke, K., Paugam, R.,
1084 Zibtsev, S., Mousseau, T. A., Wang, R., Poulter, B., Petkov, A., Yue, C., Cadule, P., Koffi, B.,
1085 Kaiser, J. W., Møller, A. P. and Classen, A. T.: Fire evolution in the radioactive forests of
1086 Ukraine and Belarus: Future risks for the population and the environment, *Ecol.*
1087 *Monogr.*, 85(1), 49–72, doi:10.1890/14-1227.1, 2015.
1088 Evangeliou, N., Zibtsev, S., Myroniuk, V., Zhurba, M., Hamburger, T., Stohl, A., Balkanski,
1089 Y., Paugam, R., Mousseau, T. A., Møller, A. P. and Kireev, S. I.: Resuspension and
1090 atmospheric transport of radionuclides due to wildfires near the Chernobyl Nuclear
1091 Power Plant in 2015: An impact assessment., *Sci. Rep.*, 6, 26062 [online] Available from:
1092 <http://www.nature.com/srep/2016/160517/srep26062/full/srep26062.html>, 2016.
1093 Fang, X., Thompson, R. L., Saito, T., Yokouchi, Y., Kim, J., Li, S., Kim, K. R., Park, S., Graziosi,
1094 F. and Stohl, A.: Sulfur hexafluoride (SF₆) emissions in East Asia determined by inverse
1095 modeling, *Atmos. Chem. Phys.*, 14(9), 4779–4791, doi:10.5194/acp-14-4779-2014,
1096 2014.
1097 Faulkner Burkhart, J., Kylling, A., Schaaf, C. B., Wang, Z., Bogren, W., Stovold, R., Solbø, S.,
1098 Pedersen, C. A. and Gerland, S.: Unmanned aerial system nadir reflectance and MODIS
1099 nadir BRDF-adjusted surface reflectances intercompared over Greenland, *Cryosphere*,
1100 11(4), 1575–1589, doi:10.5194/tc-11-1575-2017, 2017.
1101 Feng, Y., Ramanathan, V. and Kotamarthi, V. R.: Brown carbon: A significant atmospheric
1102 absorber of solar radiation, *Atmos. Chem. Phys.*, 13(17), 8607–8621, doi:10.5194/acp-
1103 13-8607-2013, 2013.
1104 Ferguson, S. A., Collins, R. L., Ruthford, J. and Fukuda, M.: Vertical distribution of
1105 nighttime smoke following a wildland biomass fire in boreal Alaska, *J. Geophys. Res.*,

1106 108(June), D23, 4743, doi:10.1029/2002JD003324, doi:10.1029/2002JD003324, 2003.
1107 Fernandez Anez, N., Garcia Torrent, J., Medic Pejic, L. and Grima Olmedo, C.: Detection of
1108 incipient self-ignition process in solid fuels through gas emissions methodology, *J. Loss*
1109 *Prev. Process Ind.*, 36, 343–351, doi:10.1016/j.jlp.2015.02.010, 2015.
1110 Flanner, M. G., Zender, C. S., Randerson, J. T. and Rasch, P. J.: Present-day climate forcing
1111 and response from black carbon in snow, *J. Geophys. Res. Atmos.*, 112(11), 1–17,
1112 doi:10.1029/2006JD008003, 2007.
1113 Flanner, M. G., Zender, C. S., Hess, P. G., Mahowald, N. M., Painter, T. H., Ramanathan, V.
1114 and Rasch, P. J.: Springtime warming and reduced snow cover from carbonaceous
1115 particles, *Atmos. Chem. Phys.*, 9, 2481–2497, doi:10.5194/acp-9-2481-2009, 2009.
1116 Forster, C., Wandinger, U., Wotawa, G., James, P., Mattis, I., Althausen, D., Simmonds, P.,
1117 O'Doherty, S., Jennings, S. G., Kleefeld, C., Schneider, J., Trickl, T., Kreipl, S., Jäger, H. and
1118 Stohl, A.: Transport of boreal forest fire emissions from Canada to Europe, *J. Geophys.*
1119 *Res.*, 106, 22887, doi:10.1029/2001JD900115, 2001.
1120 Forster, C., Stohl, A. and Seibert, P.: Parameterization of convective transport in a
1121 Lagrangian particle dispersion model and its evaluation, *J. Appl. Meteorol. Climatol.*,
1122 46(4), 403–422, doi:10.1175/JAM2470.1, 2007.
1123 Freitas, S. R., Longo, K. M., Chatfield, R., Latham, D., Silva Dias, M. a. F., Andreae, M. O.,
1124 Prins, E., Santos, J. C., Gielow, R. and Carvalho, J. a.: Including the sub-grid scale plume
1125 rise of vegetation fires in low resolution atmospheric transport models, *Atmos. Chem.*
1126 *Phys. Discuss.*, 6(6), 11521–11559, doi:10.5194/acpd-6-11521-2006, 2006.
1127 Freitas, S. R., Longo, K. M., Trentmann, J. and Latham, D.: Technical Note: Sensitivity of 1-
1128 D smoke plume rise models to the inclusion of environmental wind drag, *Atmos. Chem.*
1129 *Phys.*, 10(2), 585–594, doi:10.5194/acp-10-585-2010, 2010.
1130 French, N., Kasischke, E., Hall, R., Murphy, K., Verbyla, D., Hoy, E. and Allen, J.: Using
1131 Landsat data to assess fire and burn severity in the North American boreal forest region:
1132 an overview and summary of results, *Int. J. Wildl. Fire*, 17(4), 443–462,
1133 doi:10.1071/WF08007, 2008.
1134 Fromm, M., Bevilacqua, R., Servranckx, R., Rosen, J., Thayer, J. P., Herman, J. and Larko, D.:
1135 Pyro-cumulonimbus injection of smoke to the stratosphere: Observations and impact of
1136 a super blowup in northwestern Canada on 3-4 August 1998, *J. Geophys. Res. D Atmos.*,
1137 110(8), 1–17, doi:10.1029/2004JD005350, 2005.
1138 Giglio, L., Descloitres, J., Justice, C. O. and Kaufman, Y. J.: An enhanced contextual fire
1139 detection algorithm for MODIS, *Remote Sens. Environ.*, 87(2–3), 273–282,
1140 doi:10.1016/S0034-4257(03)00184-6, 2003.
1141 Grannas, A. M., Shepson, P. B. and Filley, T. R.: Photochemistry and nature of organic
1142 matter in Arctic and Antarctic snow, *Global Biogeochem. Cycles*, 18(1), n/a-n/a,
1143 doi:10.1029/2003GB002133, 2004.
1144 Grythe, H., Kristiansen, N. I., Groot Zwaaftink, C. D., Eckhardt, S., Ström, J., Tunved, P.,
1145 Krejci, R. and Stohl, A.: A new aerosol wet removal scheme for the Lagrangian particle
1146 model FLEXPARTv10, *Geosci. Model Dev.*, 10, 1447–1466, doi:10.5194/gmd-10-1447-
1147 2017, 2017.
1148 Hansen, J. and Nazarenko, L.: Soot climate forcing via snow and ice albedos, *Proc. Natl.*
1149 *Acad. Sci. U. S. A.*, 101(2), 423–428, doi:10.1073/pnas.2237157100, 2004.
1150 Hansen, J., Sato, M., Ruedy, R., Nazarenko, L., Lacis, A., Schmidt, G. A., Russell, G., Aleinov,
1151 I., Bauer, M., Bauer, S., Bell, N., Cairns, B., Canuto, V., Chandler, M., Cheng, Y., Del Genio, A.,
1152 Faluvegi, G., Fleming, E., Friend, A., Hall, T., Jackman, C., Kelley, M., Kiang, N., Koch, D.,
1153 Lean, J., Lerner, J., Lo, K., Menon, S., Miller, R., Minnis, P., Novakov, T., Oinas, V., Perlwitz,
1154 J., Perlwitz, J., Rind, D., Romanou, A., Shindell, D., Stone, P., Sun, S., Tausnev, N., Thresher,

1155 D., Wielicki, B., Wong, T., Yao, M. and Zhang, S.: Efficacy of climate forcings, *J. Geophys.*
1156 *Res. D Atmos.*, 110(18), 1–45, doi:10.1029/2005JD005776, 2005.

1157 Hao, W. M. and Ward, D. E.: Methane production from global biomass burning, *J.*
1158 *Geophys. Res. Atmos.*, 98(D11), 20657–20661, doi:10.1029/93JD01908, 1993.

1159 Hao, W. M., Petkov, A., Nordgren, B. L., Silverstein, R. P., Corley, R. E., Urbanski, S. P.,
1160 Evangeliou, N., Balkanski, Y. and Kinder, B.: Daily black carbon emissions from fires in
1161 Northern Eurasia from 2002 to 2013, *Geosci. Model Dev.*, 9, 4461–4474,
1162 doi:10.5194/gmd-9-4461-2016, 2016.

1163 Holben, B. N.: Characteristics of maximum-value composite images from temporal
1164 AVHRR data, *Int. J. Remote Sens.*, 7(11), 1417–1434, doi:10.1080/01431168608948945,
1165 1986.

1166 Holben, B. N., Eck, T. F., Slutsker, I., Tanré, D., Buis, J. P., Setzer, A., Vermote, E., Reagan, J.
1167 A., Kaufman, Y. J., Nakajima, T., Lavenu, F., Jankowiak, I. and Smirnov, A.: AERONET—A
1168 Federated Instrument Network and Data Archive for Aerosol Characterization, *Remote*
1169 *Sens. Environ.*, 66(1), 1–16, doi:10.1016/S0034-4257(98)00031-5, 1998.

1170 Hosseini, S., Li, Q., Cocker, D., Weise, D., Miller, A., Shrivastava, M., Miller, J. W.,
1171 Mahalingam, S., Princevac, M. and Jung, H.: Particle size distributions from laboratory-
1172 scale biomass fires using fast response instruments, *Atmos. Chem. Phys.*, 10(16), 8065–
1173 8076, doi:10.5194/acp-10-8065-2010, 2010.

1174 Hu, Y., Fernandez-Anez, N., Smith, T. E. L. and Rein, G.: Review of emissions from
1175 smouldering peat fires and their contribution to regional haze episodes, *Int. J. Wildl.*
1176 *Fire*, 27(5), 293–312, doi:10.1071/WF17084, 2018.

1177 IPCC: Climate Change 2013: The Physical Science Basis. Contribution to the Fifth
1178 Assessment Report of the Intergovernmental Panel on Climate Change., edited by T. F.
1179 Stocker, D. Qin, G.-K. Plattner, M. M. B. Tignor, S. K. Allen, J. Boschung, A. Nauels, Y. Xia, V.
1180 Bex, and P. M. Midgley, Cambridge University Press., 2013.

1181 Jacobson, M. Z.: Strong radiative heating due to the mixing state of black carbon in
1182 atmospheric aerosols, *Nature*, 409(6821), 695–697, doi:10.1038/35055518, 2001.

1183 Jedrzejek, B., Drees, B., Daniëls, F. J. A. and Hölzel, N.: Vegetation pattern of mountains in
1184 West Greenland - a baseline for long-term surveillance of global warming impacts, *Plant*
1185 *Ecol. Divers.*, 6(3–4), 405–422, doi:10.1080/17550874.2013.802049, 2013.

1186 Jo, D. S., Park, R. J., Lee, S., Kim, S. W. and Zhang, X.: A global simulation of brown carbon:
1187 Implications for photochemistry and direct radiative effect, *Atmos. Chem. Phys.*, 16(5),
1188 3413–3432, doi:10.5194/acp-16-3413-2016, 2016.

1189 Justice, C. O., Giglio, L., Korontzi, S., Owens, J., Morisette, J. T., Roy, D., Descloitres, J.,
1190 Alleaume, S., Petitcolin, F. and Kaufman, Y.: The MODIS fire products, *Remote Sens.*
1191 *Environ.*, 83(1–2), 244–262, doi:10.1016/S0034-4257(02)00076-7, 2002.

1192 Kaiser, J. W., Heil, A., Andreae, M. O., Benedetti, A., Chubarova, N., Jones, L., Morcrette, J. J.,
1193 Razingger, M., Schultz, M. G., Suttie, M. and Van Der Werf, G. R.: Biomass burning
1194 emissions estimated with a global fire assimilation system based on observed fire
1195 radiative power, *Biogeosciences*, 9(1), 527–554, doi:10.5194/bg-9-527-2012, 2012.

1196 Kato, S., Ackerman, T. P., Mather, J. H. and Clothiaux, E. E.: The k-distribution method and
1197 correlated-k approximation for a shortwave radiative transfer model, *J. Quant.*
1198 *Spectrosc. Radiat. Transf.*, 62(1), 109–121, doi:10.1016/S0022-4073(98)00075-2, 1999.

1199 Keegan, K. M., Albert, M. R., McConnell, J. R. and Baker, I.: Climate change and forest fires
1200 synergistically drive widespread melt events of the Greenland Ice Sheet, , 1–4,
1201 doi:10.1073/pnas.1405397111, 2014.

1202 Key, C. H. and Benson, N. C.: Landscape assessment: Sampling and analysis methods,
1203 USDA For. Serv. Gen. Tech. Rep. RMRS-GTR-164-CD, (June), 1–55,

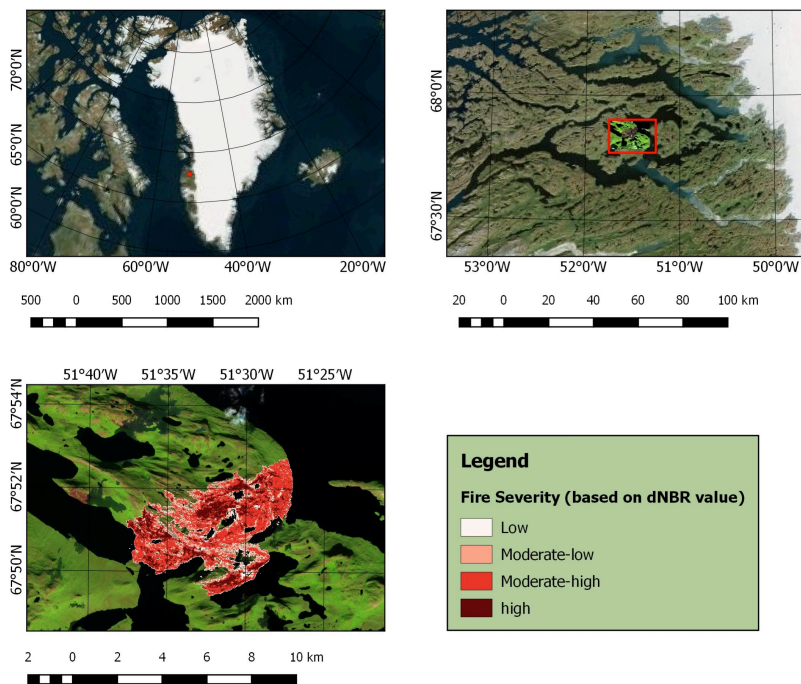
1204 doi:10.1002/app.1994.070541203, 2006.
1205 Klimont, Z., Kupiainen, K., Heyes, C., Purohit, P., Cofala, J., Rafaj, P., Borken-Kleefeld, J. and
1206 Schöpp, W.: Global anthropogenic emissions of particulate matter including black
1207 carbon, *Atmos. Chem. Phys.*, 17, 8681–8723, doi:10.5194/acp-17- 50 8681-2017, 2017.
1208 Lavoie, C. and Pellerin, S.: Fires in temperate peatlands (southern Quebec): past and
1209 recent trends, *Can. J. Bot.*, 85(3), 263–272, doi:10.1139/B07-012, 2007.
1210 Legrand, M., Preunkert, S., Jourdain, B., Guilhermet, J., Faïn, X., Alekhina, I. and Petit, J. R.:
1211 Water-soluble organic carbon in snow and ice deposited at Alpine, Greenland, and
1212 Antarctic sites: A critical review of available data and their atmospheric relevance, *Clim.
1213 Past*, 9(5), 2195–2211, doi:10.5194/cp-9-2195-2013, 2013.
1214 Legrand, M., McConnell, J., Fischer, H., Wolff, E. W., Preunkert, S., Arienzo, M., Chellman,
1215 N., Leuenberger, D., Maselli, O., Place, P., Sigl, M., Schiépach, S. and Flannigan, M.:
1216 Boreal fire records in Northern Hemisphere ice cores: A review, *Clim. Past*, 12(10),
1217 2033–2059, doi:10.5194/cp-12-2033-2016, 2016.
1218 Leino, K., Riuttanen, L., Nieminen, T., Väänänen, R., Pohja, T., Keronen, P., Järvi, L., Aalto,
1219 P. P., Virkkula, A., Kerminen, V. M., Petäjä, T., Kulmala, M., Nieminen, T., Dal Maso, M. and
1220 Virkkula, A.: Biomass-burning smoke episodes in Finland from eastern European
1221 wildfires, *Boreal Environ. Res.*, 19(x), 275–292, 2014.
1222 Lelieveld, J., Evans, J. S., Fnais, M., Giannadaki, D. and Pozzer, A.: The contribution of
1223 outdoor air pollution sources to premature mortality on a global scale., *Nature*,
1224 525(7569), 367–71, doi:10.1038/nature15371, 2015.
1225 Leung, F. Y. T., Logan, J. A., Park, R., Hyer, E., Kasischke, E., Streets, D. and Yurganov, L.:
1226 Impacts of enhanced biomass burning in the boreal forests in 1998 on tropospheric
1227 chemistry and the sensitivity of model results to the injection height of emissions, *J.
1228 Geophys. Res. Atmos.*, 112(10), 1–15, doi:10.1029/2006JD008132, 2007.
1229 Lim, H. J., Turpin, B. J., Russell, L. M. and Bates, T. S.: Organic and elemental carbon
1230 measurements during ACE-Asia suggest a longer atmospheric lifetime for elemental
1231 carbon, *Environ. Sci. Technol.*, 37(14), 3055–3061, doi:10.1021/es020988s, 2003.
1232 Limbeck, A., Kulmala, M. and Puxbaum, H.: Secondary organic aerosol formation in the
1233 atmosphere via heterogeneous reaction of gaseous isoprene on acidic particles,
1234 *Geophys. Res. Lett.*, 30(19), 4–7, doi:10.1029/2003GL017738, 2003.
1235 Long, C. M., Nascarella, M. A. and Valberg, P. A.: Carbon black vs. black carbon and other
1236 airborne materials containing elemental carbon: Physical and chemical distinctions,
1237 *Environ. Pollut.*, 181, 271–286, doi:10.1016/j.envpol.2013.06.009, 2013.
1238 Lyons, W. B., Welch, K. A. and Doggett, J. K.: Organic carbon in Antarctic snow, *Geophys.
1239 Res. Lett.*, 34(2), 2–5, doi:10.1029/2006GL028150, 2007.
1240 Magnan, G., Lavoie, M. and Payette, S.: Impact of fire on long-term vegetation dynamics
1241 of ombrotrophic peatlands in northwestern Québec, Canada, *Quat. Res.*, 77(1), 110–121,
1242 doi:http://dx.doi.org/10.1016/j.yqres.2011.10.006, 2012.
1243 Massling, A., Nielsen, I. E., Kristensen, D., Christensen, J. H., Sorensen, L. L., Jensen, B.,
1244 Nguyen, Q. T., Nøjgaard, J. K., Glasius, M. and Skov, H.: Atmospheric black carbon and
1245 sulfate concentrations in Northeast Greenland, *Atmos. Chem. Phys.*, 15(16), 9681–9692,
1246 doi:10.5194/acp-15-9681-2015, 2015.
1247 Mayer, B. and Kylling, A.: Technical note: The libRadtran software package for radiative
1248 transfer calculations - description and examples of use, *Atmos. Chem. Phys.*, 5(7), 1855–
1249 1877, doi:10.5194/acp-5-1855-2005, 2005.
1250 Mukai, H. and Ambe, Y.: Characterization of a humic acid-like brown substance in
1251 airborne particulate matter and tentative identification of its origin, *Atmos. Environ.*,
1252 20(5), 813–819, doi:https://doi.org/10.1016/0004-6981(86)90265-9, 1986.

1253 Myhre, G., Shindell, D., Bréon, F.-M., Collins, W., Fuglestedt, J., Huang, J., Koch, D.,
1254 Lamarque, J.-F., Lee, D., Mendoza, B., Nakajima, T., Robock, A., Stephens, G., Takemura, T.
1255 and Zhang, H.: Anthropogenic and Natural Radiative Forcing, in *Climate Change 2013:*
1256 *The Physical Science Basis. Contribution of Working Group I to the Fifth Assessment*
1257 *Report of the Intergovernmental Panel on Climate Change*, edited by Stocker, T.F., D. Qin,
1258 G.-K. Plattner, M. Tignor, S. K. Allen, J. Boschung, A. Nauels, Y. Xia, V. Bex, and P. M.
1259 Midgley, pp. 659–740, Cambridge University Press, Cambridge, United Kingdom and
1260 New York, NY, USA., 2013.
1261 NASA: FIRMS. Web Fire Mapper, [online] Available from:
1262 <https://firms.modaps.eosdis.nasa.gov/firemap/> (Accessed 5 September 2017a), 2017.
1263 NASA: Roundtable: The Greenland Wildfire, [online] Available from:
1264 [https://earthobservatory.nasa.gov/blogs/earthmatters/2017/08/10/roundtable-the-](https://earthobservatory.nasa.gov/blogs/earthmatters/2017/08/10/roundtable-the-greenland-wildfire/)
1265 [greenland-wildfire/](https://earthobservatory.nasa.gov/blogs/earthmatters/2017/08/10/roundtable-the-greenland-wildfire/) (Accessed 6 September 2017b), 2017.
1266 NASA: Wildfires Continue to Beleaguer Western Canada, [online] Available from:
1267 [https://www.nasa.gov/image-feature/goddard/2017/wildfires-continue-to-beleaguer-](https://www.nasa.gov/image-feature/goddard/2017/wildfires-continue-to-beleaguer-western-canada)
1268 [western-canada](https://www.nasa.gov/image-feature/goddard/2017/wildfires-continue-to-beleaguer-western-canada) (Accessed 29 October 2017c), 2017.
1269 *New Scientist Magazine: Largest ever wildfire in Greenland seen burning from space,*
1270 [online] Available from: [https://www.newscientist.com/article/2143159-largest-ever-](https://www.newscientist.com/article/2143159-largest-ever-wildfire-in-greenland-seen-burning-from-space/)
1271 [wildfire-in-greenland-seen-burning-from-space/](https://www.newscientist.com/article/2143159-largest-ever-wildfire-in-greenland-seen-burning-from-space/) (Accessed 6 September 2017), 2017.
1272 Page, S. E., Siegert, F., Rieley, J. O., Boehm, H.-D. V., Jada, A. and Limin, S.: The amount of
1273 carbon released from peat and forest fires in Indonesia during 1997, *Nature*, 420(19),
1274 61–65, doi:10.1038/nature01131, 2015.
1275 Paugam, R., Wooster, M. and Atherton, J.: Development and optimization of a wildfire
1276 plume rise model based on remote sensing data inputs – Part 2, , doi:10.5194/acpd-15-
1277 9815-2015, 2015.
1278 Pokhrel, R. P., Wagner, N. L., Langridge, J. M., Lack, D. A., Jayarathne, T., Stone, E. A.,
1279 Stockwell, C. E., Yokelson, R. J. and Murphy, S. M.: Parameterization of single-scattering
1280 albedo (SSA) and absorption Ångström exponent (AAE) with EC/OC for aerosol
1281 emissions from biomass burning, *Atmos. Chem. Phys.*, 16(15), 9549–9561,
1282 doi:10.5194/acp-16-9549-2016, 2016.
1283 Polashenski, C. M., Dibb, J. E., Flanner, M. G., Chen, J. Y., Courville, Z. R., Lai, A. M., Schauer,
1284 J. J., Shafer, M. M. and Bergin, M.: Neither dust nor black carbon causing apparent albedo
1285 decline in Greenland’s dry snow zone: Implications for MODIS C5 surface reflectance,
1286 *Geophys. Res. Lett.*, 42(21), 9319–9327, doi:10.1002/2015GL065912, 2015.
1287 Randerson, J. T., Chen, Y., Van Der Werf, G. R., Rogers, B. M. and Morton, D. C.: Global
1288 burned area and biomass burning emissions from small fires, *J. Geophys. Res.*
1289 *Biogeosciences*, 117(4), doi:10.1029/2012JG002128, 2012.
1290 Reddy, A. D., Hawbaker, T. J., Wurster, F., Zhu, Z., Ward, S., Newcomb, D. and Murray, R.:
1291 Quantifying soil carbon loss and uncertainty from a peatland wildfire using multi-
1292 temporal LiDAR, *Remote Sens. Environ.*, 170, 306–316, doi:10.1016/j.rse.2015.09.017,
1293 2015.
1294 Rémy, S., Veira, A., Paugam, R., Sofiev, M., Kaiser, J. W., Marengo, F., Burton, S. P.,
1295 Benedetti, A., Engelen, R. J., Ferrare, R. and Hair, J. W.: Two global data sets of daily fire
1296 emission injection heights since 2003, , 2921–2942, doi:10.5194/acp-17-2921-2017,
1297 2017.
1298 Restuccia, F., Ptak, N. and Rein, G.: Self-heating behavior and ignition of shale rock,
1299 *Combust. Flame*, 176, 213–219, doi:10.1016/j.combustflame.2016.09.025, 2017a.
1300 Restuccia, F., Huang, X. and Rein, G.: Self-ignition of natural fuels: Can wildfires of
1301 carbon-rich soil start by self-heating?, *Fire Saf. J.*, 91(February), 828–834,

1302 doi:10.1016/j.firesaf.2017.03.052, 2017b.
1303 von Schneidmesser, E., Schauer, J. J., Hagler, G. S. W. and Bergin, M. H.: Concentrations
1304 and sources of carbonaceous aerosol in the atmosphere of Summit, Greenland, *Atmos.*
1305 *Environ.*, 43(27), 4155–4162, doi:10.1016/j.atmosenv.2009.05.043, 2009.
1306 Seiler, W. and Crutzen, P. J.: Estimates of gross and net fluxes of carbon between the
1307 biosphere and the atmosphere from biomass burning, *Clim. Change*, 2(3), 207–247,
1308 doi:10.1007/BF00137988, 1980.
1309 SERMITSIAQ: Se billeder: Naturbrand udvikler kraftig røg, , in Danish [online] Available
1310 from: <http://sermitsiaq.ag/se-billeder-naturbrand-udvikler-kraftig-roeg> (Accessed 6
1311 September 2017), 2017.
1312 Shetler, G., Turetsky, M. R., Kane, E. and Kasischke, E.: Sphagnum mosses limit total
1313 carbon consumption during fire in Alaskan black spruce forests, *Can. J. For. Res.*, 38(8),
1314 2328–2336, doi:10.1139/X08-057, 2008.
1315 Shi, Y., Matsunaga, T., Saito, M., Yamaguchi, Y. and Chen, X.: Comparison of global
1316 inventories of CO₂ emissions from biomass burning during 2002–2011 derived from
1317 multiple satellite products, *Environ. Pollut.*, 206, 479–487,
1318 doi:10.1016/j.envpol.2015.08.009, 2015.
1319 Skeie, R. B., Berntsen, T., Myhre, G., Pedersen, C. A., Ström, J., Gerland, S. and Ogren, J. A.:
1320 Black carbon in the atmosphere and snow, from pre-industrial times until present,
1321 *Atmos. Chem. Phys.*, 11(14), 6809–6836, doi:10.5194/acp-11-6809-2011, 2011.
1322 Smirnov, N. S., Korotkov, V. N. and Romanovskaya, A. A.: Black carbon emissions from
1323 wildfires on forest lands of the Russian Federation in 2007–2012, *Russ. Meteorol.*
1324 *Hydrol.*, 40(7), 435–442, doi:10.3103/S1068373915070018, 2015.
1325 Stamnes, K., Tsay, S.-C., Wiscombe, W. and Jayaweera, K.: Numerically stable algorithm
1326 for discrete-ordinate-method radiative transfer in multiple scattering and emitting
1327 layered media, *Appl. Opt.*, 27(12), 2502, doi:10.1364/AO.27.002502, 1988.
1328 Stendel, M., Christensen, J. H. and Petersen, D.: Arctic Climate and Climate Change with a
1329 Focus on Greenland, *Adv. Ecol. Res.*, 40(07), 13–43, doi:10.1016/S0065-
1330 2504(07)00002-5, 2008.
1331 Stockwell, C. E., Jayarathne, T., Cochrane, M. A., Ryan, K. C., Putra, E. I., Saharjo, B. H.,
1332 Nurhayati, A. D., Albar, I., Blake, D. R., Simpson, I. J., Stone, E. A. and Yokelson, R. J.: Field
1333 measurements of trace gases and aerosols emitted by peat fires in Central Kalimantan,
1334 Indonesia, during the 2015 El Niño, *Atmos. Chem. Phys.*, 16(18), 11711–11732,
1335 doi:10.5194/acp-16-11711-2016, 2016.
1336 Stohl, A., Forster, C., Frank, A., Seibert, P. and Wotawa, G.: Technical note: The Lagrangian
1337 particle dispersion model FLEXPART version 6.2, *Atmos. Chem. Phys.*, 5(9), 2461–2474,
1338 doi:10.5194/acp-5-2461-2005, 2005.
1339 Stohl, A., Andrews, E., Burkhardt, J. F., Forster, C., Herber, A., Hoch, S. W., Kowal, D.,
1340 Lunder, C., Mefford, T., Ogren, J. A., Sharma, S., Spichtinger, N., Stebel, K., Stone, R., Ström,
1341 J., Tørseth, K., Wehrli, C. and Yttri, K. E.: Pan-Arctic enhancements of light absorbing
1342 aerosol concentrations due to North American boreal forest fires during summer 2004, *J.*
1343 *Geophys. Res. Atmos.*, 111(22), 1–20, doi:10.1029/2006JD007216, 2006.
1344 Stohl, A., Berg, T., Burkhardt, J. F., Fjærraa, A. M., Forster, C., Herber, A., Hov, Ø., Lunder, C.,
1345 McMillan, W. W., Oltmans, S., Shiobara, M., Simpson, D., Solberg, S., Stebel, K., Ström, J.,
1346 Tørseth, K., Treffeisen, R., Virkkunen, K. and Yttri, K. E.: Arctic smoke – record
1347 high air pollution levels in the European Arctic due to agricultural fires in Eastern
1348 Europe in spring 2006, *Atmos. Chem. Phys.*, 7(2), 511–534, doi:10.5194/acp-7-511-
1349 2007, 2007.
1350 Stohl, A., Prata, A. J., Eckhardt, S., Clarisse, L., Durant, A., Henne, S., Kristiansen, N. I.,

1351 Minikin, A., Schumann, U., Seibert, P., Stebel, K., Thomas, H. E., Thorsteinsson, T., Tørseth,
1352 K. and Weinzierl, B.: Determination of time-and height-resolved volcanic ash emissions
1353 and their use for quantitative ash dispersion modeling: The 2010 Eyjafjallajökull
1354 eruption, *Atmos. Chem. Phys.*, 11(9), 4333–4351, doi:10.5194/acp-11-4333-2011, 2011.
1355 Stohl, A., Klimont, Z., Eckhardt, S., Kupiainen, K., Shevchenko, V. P., Kopeikin, V. M. and
1356 Novigatsky, A. N.: Black carbon in the Arctic: The underestimated role of gas flaring and
1357 residential combustion emissions, *Atmos. Chem. Phys.*, 13(17), 8833–8855,
1358 doi:10.5194/acp-13-8833-2013, 2013.
1359 Stroeve, J., Box, J. E., Gao, F., Liang, S., Nolin, A. and Schaaf, C.: Accuracy assessment of the
1360 MODIS 16-day albedo product for snow: Comparisons with Greenland in situ
1361 measurements, *Remote Sens. Environ.*, 94(1), 46–60, doi:10.1016/j.rse.2004.09.001,
1362 2005.
1363 Sunderman, S. O. and Weisberg, P. J.: Remote sensing approaches for reconstructing fire
1364 perimeters and burn severity mosaics in desert spring ecosystems, *Remote Sens.*
1365 *Environ.*, 115(9), 2384–2389, doi:10.1016/j.rse.2011.05.001, 2011.
1366 Turetsky, M. R., Donahue, W. F. and Benscoter, B. W.: Experimental drying intensifies
1367 burning and carbon losses in a northern peatland, *Nat. Commun.*, 2, 514,
1368 doi:10.1038/ncomms1523, 2011.
1369 Turetsky, M. R., Benscoter, B., Page, S., Rein, G., van der Werf, G. R. and Watts, A.: Global
1370 vulnerability of peatlands to fire and carbon loss, *Nat. Geosci.*, 8(1), 11–14,
1371 doi:10.1038/ngeo2325, 2014.
1372 Urbanski, S. P., Hao, W. M. and Nordgren, B.: The wildland fire emission inventory:
1373 Western United States emission estimates and an evaluation of uncertainty, *Atmos.*
1374 *Chem. Phys.*, 11(24), 12973–13000, doi:10.5194/acp-11-12973-2011, 2011.
1375 Wandji Nyamsi, W., Arola, A., Blanc, P., Lindfors, a. V., Cesnulyte, V., Pitkänen, M. R. a. and
1376 Wald, L.: Technical Note: A novel parameterization of the transmissivity due to ozone
1377 absorption in the distribution method and correlated approximation of Kato et al.
1378 (1999) over the UV band, *Atmos. Chem. Phys.*, 15(13), 7449–7456, doi:10.5194/acp-15-
1379 7449-2015, 2015.
1380 Warren, S. G.: Can black carbon in snow be detected by remote sensing?, *J. Geophys. Res.*
1381 *Atmos.*, 118(2), 779–786, doi:10.1029/2012JD018476, 2013.
1382 Wieder, R. K., Scott, K. D., Kamminga, K., Vile, M. A., Vitt, D. H., Bone, T., Xu, B., Benscoter,
1383 B. W. and Bhatti, J. S.: Postfire carbon balance in boreal bogs of Alberta, Canada, *Glob.*
1384 *Chang. Biol.*, 15(1), 63–81, doi:10.1111/j.1365-2486.2008.01756.x, 2009.
1385 Winiger, P., Andersson, A., Eckhardt, S., Stohl, A., Semiletov, I. P., Dudarev, O. V., Charkin,
1386 A., Shakhova, N., Klimont, Z., Heyes, C. and Gustafsson, Ö.: Siberian Arctic black carbon
1387 sources constrained by model and observation, *Proc. Natl. Acad. Sci.*, 114(7), E1054–
1388 E1061, doi:10.1073/pnas.1613401114, 2017.
1389 Winker, D. M., Vaughan, M. A., Omar, A., Hu, Y., Powell, K. A., Liu, Z., Hunt, W. H. and
1390 Young, S. A.: Overview of the CALIPSO mission and CALIOP data processing algorithms, *J.*
1391 *Atmos. Ocean. Technol.*, 26(11), 2310–2323, doi:10.1175/2009JTECHA1281.1, 2009.
1392 Wu, D., Huang, X., Norman, F., Verplaetsen, F., Berghmans, J. and Van Den Bulck, E.:
1393 Experimental investigation on the self-ignition behaviour of coal dust accumulations in
1394 oxy-fuel combustion system, *Fuel*, 160, 245–254, doi:10.1016/j.fuel.2015.07.050, 2015.
1395 Wu, G. M., Cong, Z. Y., Kang, S. C., Kawamura, K., Fu, P. Q., Zhang, Y. L., Wan, X., Gao, S. P.
1396 and Liu, B.: Brown carbon in the cryosphere: Current knowledge and perspective, *Adv.*
1397 *Clim. Chang. Res.*, 7(1–2), 82–89, doi:10.1016/j.accre.2016.06.002, 2016.
1398 Zhuravleva, T. B., Kabanov, D. M., Nasrtdinov, I. M., Russkova, T. V., Sakerin, S. M.,
1399 Smirnov, A. and Holben, B. N.: Radiative characteristics of aerosol during extreme fire

1400 event over Siberia in summer 2012, Atmos. Meas. Tech., 10(1), 179–198,
1401 doi:10.5194/amt-10-179-2017, 2017.
1402
1403

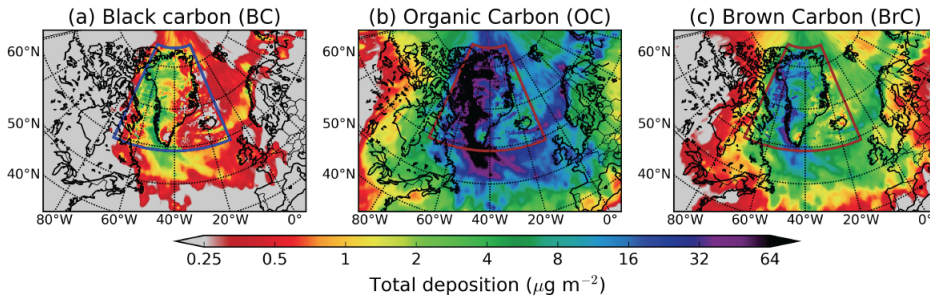


1405
 1406 **Figure 1.** Map of Greenland (upper left) and zoomed map marked with fire location (upper
 1407 right and burned area classification (bottom) in terms of fire severity according to Sentinel 2A
 1408 images for fires burning in Greenland in August 2017. To delineate fire perimeters, both
 1409 Landsat 8 OLI and Sentinel 1A – 2A data were used ([Table 1](#)).

1410

Nikolaos Evangeliou 5/12/2018 14:38
 Deleted: Table 1

CUMULATIVE DEPOSITION (31 August 2017)



1412

1413 **Figure 2.** Total (wet and dry) deposition of (a) BC, (b) OC and (c) BrC (in $\mu\text{g m}^{-2}$) from the
1414 Greenland fires until 31 August 2017. The colored rectangle depicts the nested high-
1415 resolution domain.

1416

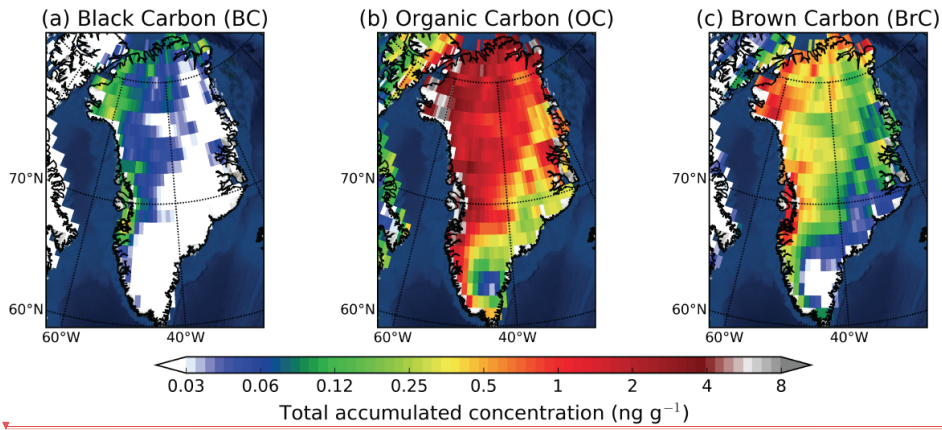
Nikolaos Evangeliou 25/10/2018 22:26

Deleted: (a) Vertical distribution of BC concentrations from the fires in the area of Greenland in summer 2017 as a function of time. (b)

Nikolaos Evangeliou 8/6/2018 10:38

Deleted: n

SNOW CONCENTRATIONS BASED ON SNOW ACCUMULATION FROM ECMWF



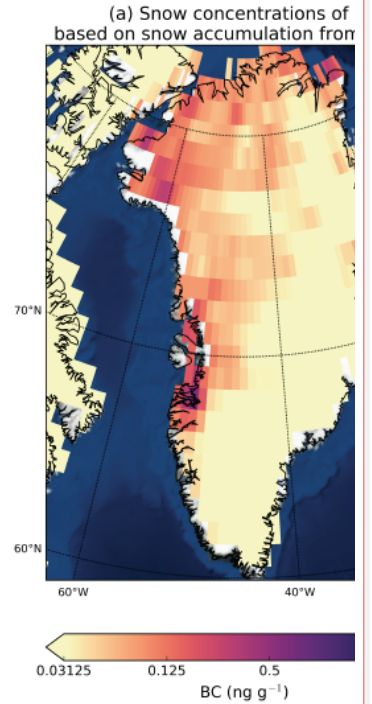
1422

1423 **Figure 3.** Calculated snow concentrations of (a) BC, (b) OC and (c) BrC over Greenland
 1424 based on the modeled deposition and the snow precipitation (large scale and convective)
 1425 adopted from the operational ECMWF data that were used in our simulation (see section 2.3).

1426

Nikolaos Evangeliou 25/10/2018 23:27

Deleted:



Nikolaos Evangeliou 25/10/2018 23:27

Deleted: (a)

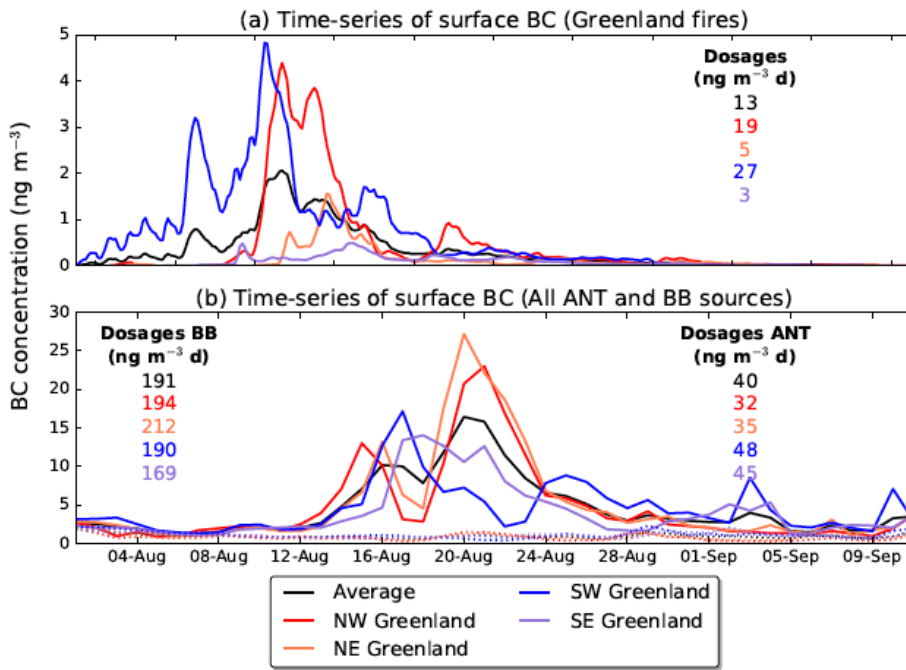
Nikolaos Evangeliou 25/10/2018 23:28

Deleted: in

Nikolaos Evangeliou 25/10/2018 23:28

Deleted: (b) Dry to total deposition ratio of BC from the 2017 peat fires over Greenland.

1433



1434

1435 **Figure 4.** (a) Time-series of surface BC concentrations in Northwestern, Northeastern,
 1436 Southwestern and Southeastern Greenland from the summer 2017 fires in Western Greenland.
 1437 (b) Time-series of surface BC concentrations in Northwestern, Northeastern, Southwestern
 1438 and Southeastern Greenland from global anthropogenic (ANT, dashed lines) and biomass
 1439 burning (BB, solid lines) emissions for the same period. The numbers represent the respective
 1440 dosages (time-integrated concentrations) for the time period shown. The color codes are
 1441 reported in the legend.

1442

Nikolaos Evangeliou 6/6/2018 17:47

CONTRIBUTION FROM BI

Northwestern Greenland No

BB 30.9 ng m⁻³

Northwestern Greenland No

ANT 4.5 ng m⁻³

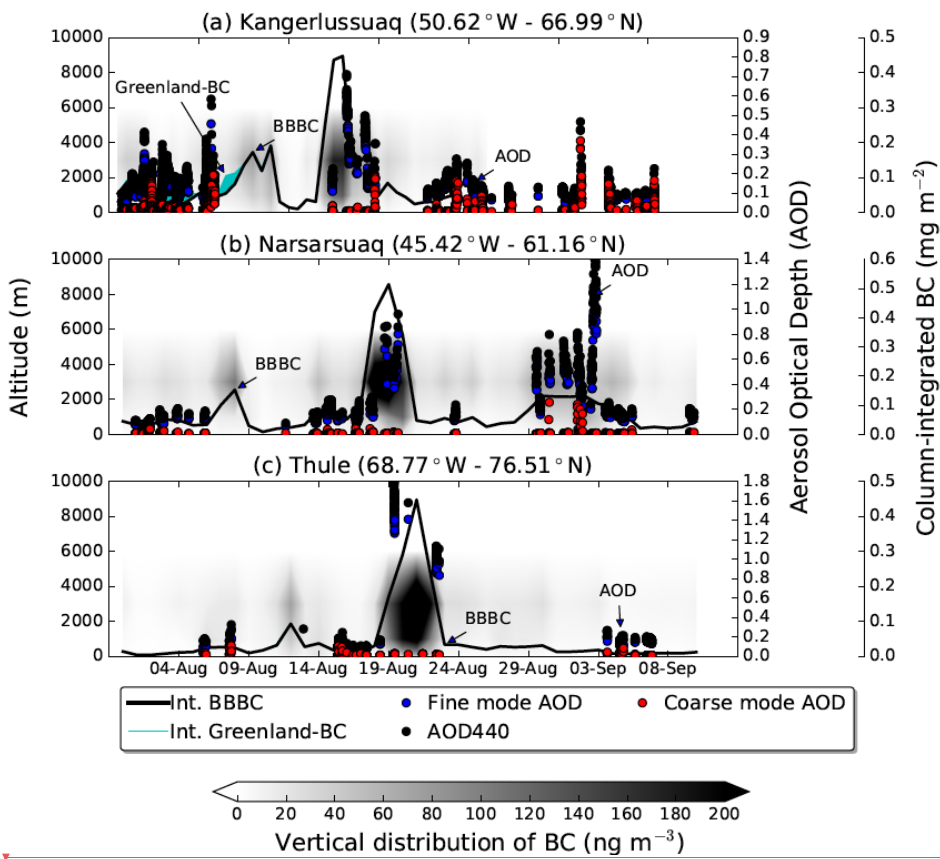
Deleted:
 Unknown
 Formatted: Font:Times New Roman, 12 pt, Not Bold, Font color: Auto
 Unknown
 Formatted: Font:Times New Roman, 12 pt, Font color: Auto

Andreas Stohl 17/6/2018 00:59
Deleted: summed

Andreas Stohl 17/6/2018 01:00
Deleted: and each

Andreas Stohl 17/6/2018 01:00
Deleted: corresponds to

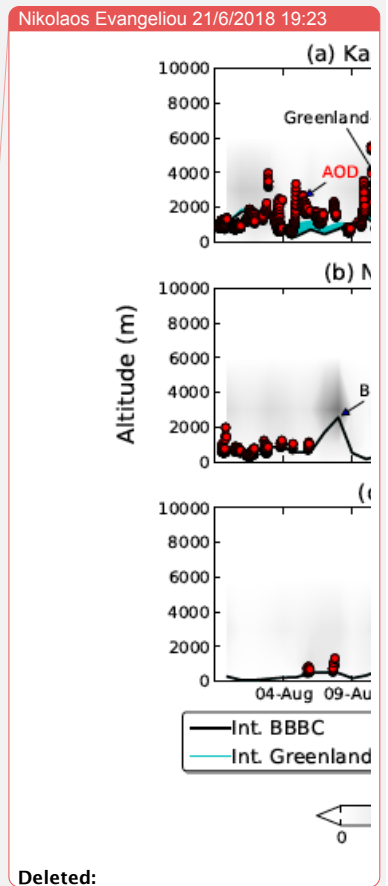
Nikolaos Evangeliou 6/6/2018 17:46
Moved down [1]: Average contribution of biomass burning (upper panels) and anthropogenic emissions (lower panels) to surface concentrations of BC in Northwestern, Northeastern, Southwestern and Southeastern Greenland (in ng m⁻³ per grid cell). Numbers (in red) represent total concentrations in the studied domain, obtained by spatial integration over all source grid cells. Receptor areas in Greenland are highlighted by pink boxes.



1457

1458 **Figure 5.** Contour plot of the vertical distribution of simulated BC (altitude a.g.l. shown on
 1459 left y-axis) as a function of time (x-axis) and time-series of column-integrated simulated BC
 1460 (extended right axis) from fires burning outside Greenland (black line) and Greenland fires
 1461 (cyan stacked area). Column-integrated BC from anthropogenic sources was extremely small
 1462 and it is not plotted here. Time-series for fine mode (blue) and coarse (red) AOD at 500 nm
 1463 and total AOD at 400 nm (black) correspond to the right y-axis. The three panels show results
 1464 for stations (a) Kangerlussuaq, (b) Narsarsuaq and (c) Thule (sorted from the closest to the
 1465 farthest station).

1466



Deleted:

Nikolaos Evangeliou 21/6/2018 19:15

Deleted: Also shown are t

Nikolaos Evangeliou 21/6/2018 19:19

Deleted: of AOD measurements

Nikolaos Evangeliou 21/6/2018 19:13

Deleted: black

Nikolaos Evangeliou 21/6/2018 19:19

Deleted: ,

Nikolaos Evangeliou 21/6/2018 19:14

Deleted: all (blue) aerosol particles

Nikolaos Evangeliou 21/6/2018 19:20

Deleted: at 500

Nikolaos Evangeliou 21/6/2018 19:15

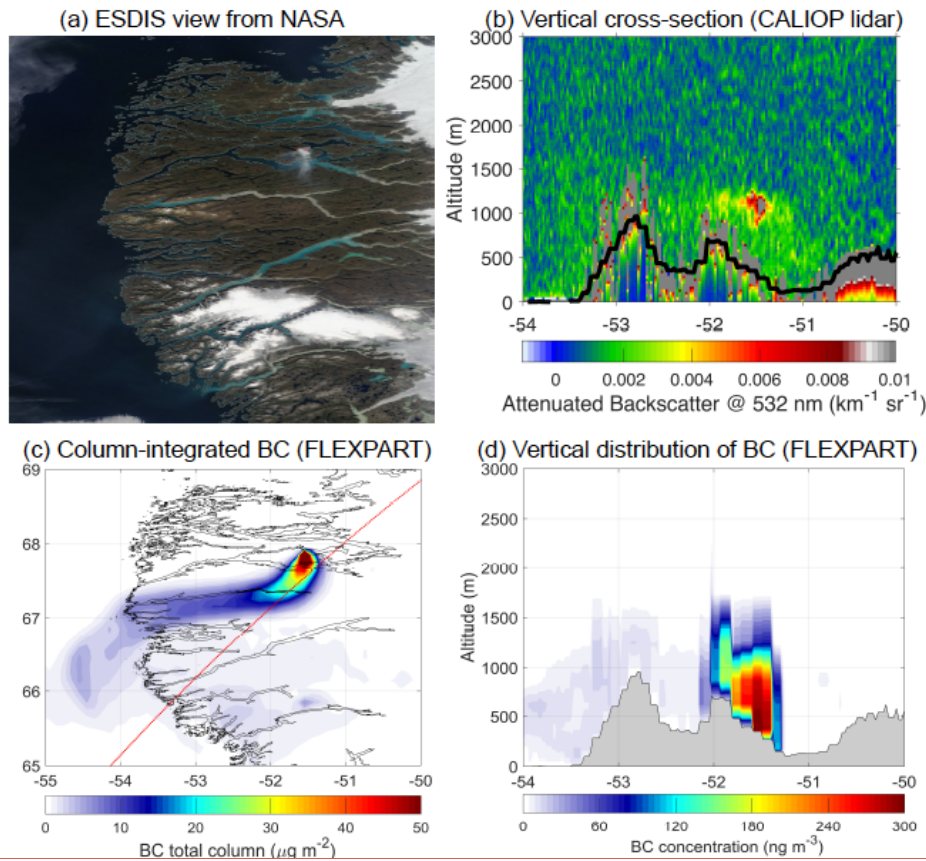
Deleted: (

Nikolaos Evangeliou 21/6/2018 19:15

Deleted:)

Nikolaos Evangeliou 21/6/2018 19:15

Deleted:

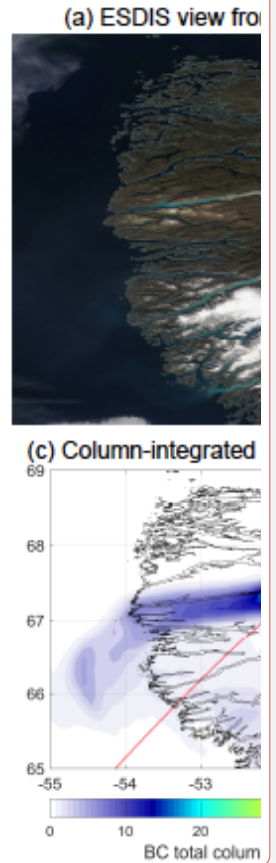


1478

1479 **Figure 6.** (a) Worldview application from the NASA/Goddard Space Flight Center
 1480 Science Data and Information System (ESDIS) project on 14 August 2017. (b) Vertical cross-
 1481 section along satellite's route (red line in c) of total attenuated backscatter at a wavelength of
 1482 532 nm obtained from the CALIOP lidar on 14 August 2017 at 6 UTC (black line denotes the
 1483 orography of the area). (c) Column-integrated BC concentration simulated with FLEXPART
 1484 (read line shows the path of the satellite). (d) Vertical distribution of BC concentrations with
 1485 longitude as seen with FLEXPART (grey area denotes the orography of the area).

1486

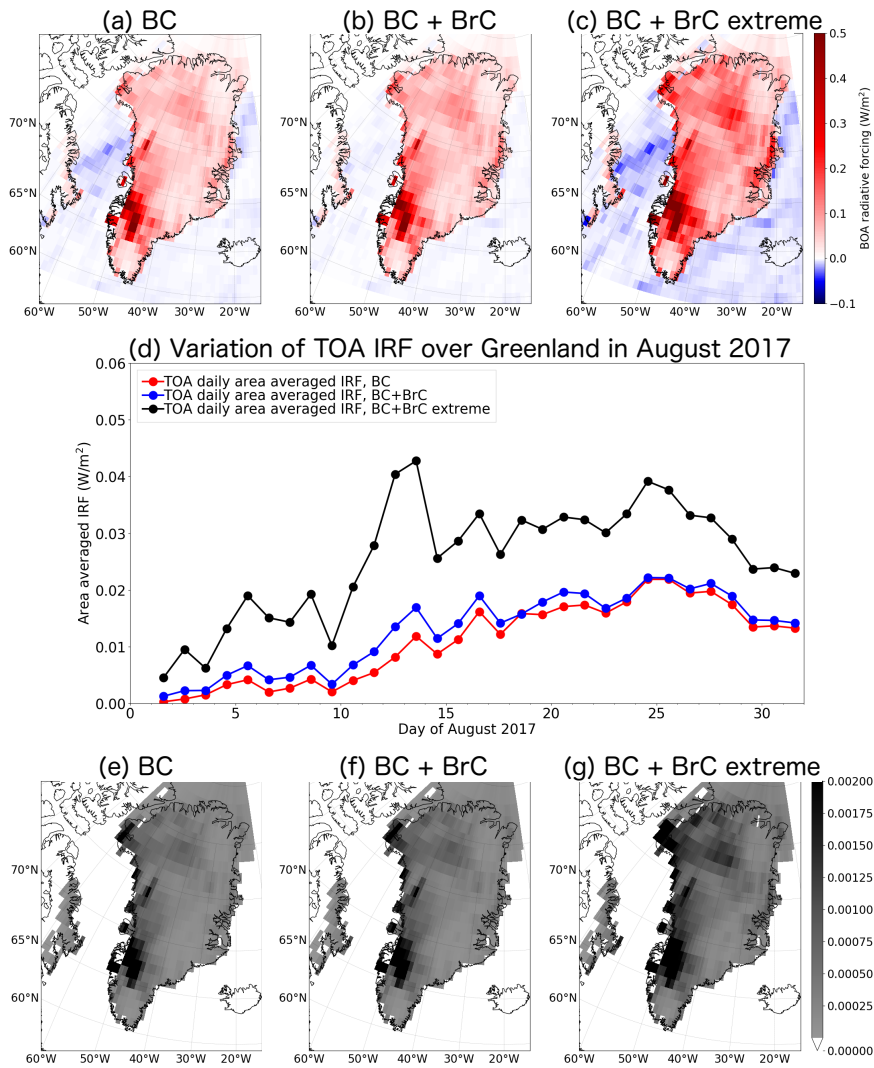
Nikolaos Evangeliou 20/6/2018 13:53



Deleted:

Unknown

Formatted: Font:Times New Roman, 12 pt, Not Bold, Font color: Auto



1488

1489 **Figure 7.** The instantaneous direct BOA RF due to (a) BC only, (b) BC and BrC, and (c) BC
 1490 and BrC when OC was assumed to be all BrC (extreme case) from the Greenland fire for
 1491 cloudy conditions on 31 August, 2017. (d) Daily variation of the TOA IRF over Greenland in
 1492 August 2017 for the three studied scenarios. Albedo reduction at 550 nm due to (e) BC only,
 1493 (f) BC and BrC, and (g) BC and BrC when OC was assumed to be all BrC (extreme case).
 1494 Note that the maximum albedo change due to deposited smoke is 0.00585 (BC only), 0.00590
 1495 (BC+BrC) and 0.00670 (BC+BrC extreme).

Unknown
 Formatted: Font:Times New Roman, 12 pt, Font color: Auto

Nikolaos Evangeliou 4/12/2018 14:27
 Formatted: Caption, Justified, Line spacing: 1.5 lines

Nikolaos Evangeliou 4/12/2018 14:22
 Deleted: (a) The instantaneous direct BOA RF due to BC from the Greenland fires for cloudless and (b) cloudy conditions on 31 August, and (c) snow albedo reduction. (d) Temporal variation of the TOA IRF over Greenland in August 2017. .

1502 SUPPLEMENTARY FIGURE LEGENDS

1503

1504 [Figure S 1. Annual number of active fires over Greenland during the last 17 years as seen](#)
1505 [from NASA's MODIS satellite \(product MSC14DL\).](#)

1506

1507 [Figure S 2. Fire dynamics in Greenland for the August 2017 fires according to MODIS](#)
1508 [\(magenta dots show active fire hot spots from the MODIS MCD14DL product\). Locations of](#)
1509 [stations with AOD measurements from AERONET are also shown.](#)

1510

1511 [Figure S 3. Median injection heights \(km above sea level – ASL; left panel\) and distribution](#)
1512 [of longitudinally integrated burned biomass \(Tg\) as a function of injection altitude \(right](#)
1513 [panel\) calculated by PRMv2 for the period between 31 July and 21 August 2017.](#)

1514 [Figure S 4. Dry to total deposition ratio \(example for BC\) from the 2017 peat fires over](#)
1515 [Greenland.](#)

1516

1517 [Figure S 5. Relative standard deviation of deposited mass \(example for BC\) for different](#)
1518 [assumed size distributions normalized against the results from our reference size distribution](#)
1519 [with a logarithmic mean diameter of 0.25 \$\mu\text{m}\$. Particle size distributions with aerodynamic](#)
1520 [mean diameters of 0.1, 0.25, 0.5, 1, 2, 4, 8 \$\mu\text{m}\$ and a logarithmic standard deviation of 0.3](#)
1521 [were simulated.](#)

1522

1523 [Figure S 6. Footprint emissions sensitivities for Northwestern, Northeastern, Southwestern](#)
1524 [and Southeastern Greenland for the period 31 July to 31 August 2017. Active fires from](#)
1525 [NASA's MODIS MCD14DL product are shown with red dots.](#)

1526

1527 [Figure S 7. Average contribution of biomass burning \(upper panels\) and anthropogenic](#)
1528 [emissions \(lower panels\) to surface concentrations of \(a\) BC and \(b\) OC in Northwestern,](#)
1529 [Northeastern, Southwestern and Southeastern Greenland \(in \$\text{ng m}^{-3}\$ per grid cell\). Numbers \(in](#)
1530 [red\) represent total concentrations in the studied domain, obtained by spatial integration over](#)
1531 [all source grid cells. Receptor areas in Greenland are highlighted by pink boxes.](#)

1532

Nikolaos Evangeliou 26/10/2018 10:38

Deleted: 21

Nikolaos Evangeliou 26/10/2018 10:38

Deleted: 32

Nikolaos Evangeliou 26/10/2018 10:38

Deleted: 4

Nikolaos Evangeliou 26/10/2018 10:38

Deleted: 5

Nikolaos Evangeliou 26/10/2018 10:38

Deleted: 64

Nikolaos Evangeliou 6/6/2018 17:46

Moved (insertion) [1]

Nikolaos Evangeliou 6/6/2018 17:46

Deleted: (a) Time-series of surface BC concentrations in Northwestern, Northeastern, Southwestern and Southeastern Greenland from the summer 2017 fires in Western Greenland. (b) Time-series of surface BC concentrations in Northwestern, Northeastern, Southwestern and Southeastern Greenland from global anthropogenic (ANT) and biomass burning (BB) emissions for the same period. The numbers represent the respective dosages integrated for the time period shown and each color corresponds to the legend.

1550 **Figure S 8.** (a) The single scattering albedo (SSA) of BC as a function of wavelength for
1551 various modified combustion efficiencies (MCE). The star and dot marked lines are from the
1552 parameterization of Pokhrel et al. (2016). (b) The IRF as a function of BC deposited on the
1553 Ice Sheet. The calculations were made for cloudless conditions with a snow-covered surface
1554 for noon on 31 August 2017 at 65°N.

Nikolaos Evangeliou 15/6/2018 15:13

Formatted: Caption, Justified, Line
spacing: 1.5 lines

Nikolaos Evangeliou 26/10/2018 10:38

Deleted: 7

Table 1. Start and end date of releases, source of data, type of sensor, burned area and daily increment of burned area, fuel consumption and calculated BC emissions from Eq. 1 during the Greenland fires in 2017. Total numbers for burned area, fuel consumption and BC emissions are highlighted in bold.

Start	End	Source of RS data	Type of sensor	Burned area (ha)	Increment of burned area (ha)	Fuel consumption (t C)	BC emissions (kg)	OC emissions (kg)	BrC emissions (kg)
31/07/17	02/08/17	Sentinel 2A	MSI	304	304	15176	3035	94543	18211
02/08/17	03/08/17	Landsat 8 OLI	MSI	428	125	6247	1249	38916	7496
03/08/17	04/08/17	Sentinel 1A	SAR	588	160	7980	1596	49712	9575
04/08/17	05/08/17	Sentinel 1A	SAR	740	152	7621	1524	47479	9145
05/08/17	07/08/17	Sentinel 2A	MSI	1100	359	17966	3593	111925	21559
07/08/17	08/08/17	Sentinel 2A	MSI	1314	214	10706	2141	66698	12847
08/08/17	12/08/17	Landsat 8 OLI	MSI	1868	554	27714	5543	172658	33257
12/08/17	14/08/17	Sentinel 1A	SAR	2005	136	6817	1363	42470	8180
14/08/17	15/08/17	Sentinel 1A	SAR	2169	165	8244	1649	51363	9893
15/08/17	16/08/17	Sentinel 1A	SAR	2209	40	1998	400	12444	2397
16/08/17	19/08/17	Sentinel 1A	SAR	2254	44	2213	443	13784	2655
19/08/17	21/08/17	Sentinel 2A	MSI	2345	92	4579	916	28530	5495
TOTAL					2345	117259	23452	730524	140711

RS - Remote Sensing

MSI - Multispectral Images

SAR - Synthetic Aperture RADAR

Page 2: [1] Deleted	Nikolaos Evangeliou	04/12/2018 14:52
---------------------	---------------------	------------------

BC

Page 2: [1] Deleted	Nikolaos Evangeliou	04/12/2018 14:52
---------------------	---------------------	------------------

BC

Page 2: [2] Deleted	Andreas Stohl	05/12/2018 12:53
---------------------	---------------	------------------

,

Page 2: [2] Deleted	Andreas Stohl	05/12/2018 12:53
---------------------	---------------	------------------

,

Page 2: [3] Deleted	Nikolaos Evangeliou	04/12/2018 14:54
---------------------	---------------------	------------------

BC

Page 2: [3] Deleted	Nikolaos Evangeliou	04/12/2018 14:54
---------------------	---------------------	------------------

BC

Page 2: [3] Deleted	Nikolaos Evangeliou	04/12/2018 14:54
---------------------	---------------------	------------------

BC

Page 2: [3] Deleted	Nikolaos Evangeliou	04/12/2018 14:54
---------------------	---------------------	------------------

BC

Page 2: [4] Deleted	Nikolaos Evangeliou	04/12/2018 14:55
---------------------	---------------------	------------------

BC

Page 2: [4] Deleted	Nikolaos Evangeliou	04/12/2018 14:55
---------------------	---------------------	------------------

BC

Page 2: [5] Deleted	Nikolaos Evangeliou	04/12/2018 14:57
---------------------	---------------------	------------------

um values

Page 2: [5] Deleted	Nikolaos Evangeliou	04/12/2018 14:57
---------------------	---------------------	------------------

um values

Page 2: [5] Deleted	Nikolaos Evangeliou	04/12/2018 14:57
---------------------	---------------------	------------------

um values

Page 2: [5] Deleted	Nikolaos Evangeliou	04/12/2018 14:57
---------------------	---------------------	------------------

um values

Page 2: [5] Deleted	Nikolaos Evangeliou	04/12/2018 14:57
---------------------	---------------------	------------------

um values

Page 2: [5] Deleted Nikolaos Evangeliou 04/12/2018 14:57

um values

Page 2: [5] Deleted Nikolaos Evangeliou 04/12/2018 14:57

um values

Page 2: [5] Deleted Nikolaos Evangeliou 04/12/2018 14:57

um values

Page 2: [5] Deleted Nikolaos Evangeliou 04/12/2018 14:57

um values

Page 2: [5] Deleted Nikolaos Evangeliou 04/12/2018 14:57

um values

Page 2: [5] Deleted Nikolaos Evangeliou 04/12/2018 14:57

um values

Page 2: [5] Deleted Nikolaos Evangeliou 04/12/2018 14:57

um values

Page 2: [5] Deleted Nikolaos Evangeliou 04/12/2018 14:57

um values

Page 9: [6] Deleted Andreas Stohl 17/06/2018 14:45

RF was calculated at the top and bottom of the atmosphere at $1^\circ \times 1^\circ$ resolution.

Page 16: [7] Deleted Nikolaos Evangeliou 20/06/2018 14:01

Another cloud of enhanced attenuated backscatter is evident at 4–5 km altitude between 50.5°E and 48.5°E . This mid-tropospheric plume was not studied but is likely due to aerosol transport from the North American fires. These large wildfires are eager to lift smoke at stratospheric altitudes as a result of super-cell convection and they have alreadySmoke from these fires was already shown to be present as such altitudes in Greenland during the study period (see Figure 5Figure 5). As shown in

Page 16: [8] Deleted Andreas Stohl 17/06/2018 09:59

Effect on snow and ice surfaces

1.1

Page 16: [9] Deleted	Andreas Stohl	17/06/2018 10:17
----------------------	---------------	------------------

The bottom of the atmosphere (BOA) instantaneous radiative forcing (IRF) due to the Greenland fires

Page 16: [10] Deleted	Nikolaos Evangeliou	06/06/2018 11:49
-----------------------	---------------------	------------------

at the bottom of the atmosphere (BOA)

Page 16: [11] Deleted	Nikolaos Evangeliou	03/12/2018 13:58
-----------------------	---------------------	------------------

, both for cloudless (Fig. 7a) and cloudy conditions (Fig. 7b)

Page 17: [12] Deleted	Nikolaos Evangeliou	06/06/2018 11:52
-----------------------	---------------------	------------------

For IRF at the top of the atmosphere (TOA), the corresponding values are 0.59 W m^{-2} and 0.03 W m^{-2} .

Page 17: [13] Deleted	Nikolaos Evangeliou	04/12/2018 13:37
-----------------------	---------------------	------------------

In addition the daily averaged IRF is shown (green line).

Page 17: [14] Deleted	Andreas Stohl	17/06/2018 11:26
-----------------------	---------------	------------------

The blue line in Figure 7db shows the value for the pixel with maximum IRF.

Page 17: [15] Deleted	Andreas Stohl	05/12/2018 13:22
-----------------------	---------------	------------------

IRF or with the BC+BrC IRF in the extreme scenario (all OC is BrC)